Larhyss Journal, ISSN 1112-3680, n°64, Dec 2025, pp. 445-516

HIGHLY ACCURATE EXPLICIT RATIONAL APPROXIMATIONS FOR THE NORMAL FLOW DEPTH PROBLEM IN RECTANGULAR CHANNELS USING MANNING'S EQUATION

ACHOUR B.[1*], AMARA L.[2]

[1] Professor, Research Laboratory in Subterranean and Surface Hydraulics (LARHYSS), University of Biskra, PO Box 145 RP, Biskra, Algeria
[2] Associate Professor, Department of Civil Engineering and Hydraulics, Faculty of Science and Technology, University of Jijel, PO Box 98, Ouled Aissa, Jijel, Algeria

(*) bachir.achour@larhyss.net

Research Article – Available at http://larhyss.net/ojs/index.php/larhyss/index
Received November 2, 2024, Received in revised form September 11, 2025, Accepted September 15, 2025

ABSTRACT

This paper addresses the classical normal depth problem in rectangular channels governed by Manning's implicit equation. It proposes and evaluates a set of nine high-accuracy explicit and rational approximation models aimed at estimating the dimensionless normal flow depth variable with exceptional accuracy across the full admissible flow domain.

After presenting the exact solution to the transcendental Manning's equation, the study develops a hierarchy of eight increasingly accurate explicit approximate models.

First, the classical Lagrange-Burmann series expansion is revisited and shown to diverge even in the practical restricted domain of the dimensionless discharge parameter $M \in [0, 1.6]$, disqualifying it as a reliable approximation. Similarly, models based on Laguerre and Legendre polynomials are examined and found inappropriate: the Laguerre model lacks orthogonality over the finite domain, while the Legendre model, despite ensuring orthogonality, relies on a normalized variable that leads to poor accuracy, with relative errors reaching up to 55% for low values of *M*.

The first rational approach leverages an accurate Padé surrogate model, achieving a maximum deviation below 0.000045%.

The Adaptive Antoulas-Anderson (AAA) rational approximation further improves accuracy, yielding a deviation under 10^{-7} %.

A third solution based on Chebyshev polynomial approximation maintains a maximum relative deviation below 0.00035%. Building upon this, a Lawson-refined AAA model significantly enhances performance with a deviation below 3.7×10^{-9} %.

To preserve monotonicity and shape, a Piecewise Cubic Hermite Interpolating Polynomial (PCHIP) is adopted, maintaining an absolute deviation under 1.7×10^{-5} %.

The Achour and Amara accurate two-piece rational model (Model I) demonstrates outstanding performance, producing a deviation of just 0.0000004% in the lower domain and sub-1.32×10^{-6} % in the upper domain.

In parallel, an iterated-perturbation analytical model by Amara and Achour yields a robust maximum deviation under 0.006%.

A highly accurate one-piece [3/3] rational model by Achour and Amara is also developed, achieving a deviation below 0.00016%.

Lastly, a rational two-piece [2/2] model (Model II) offers deviations of 0.0062% for the lower piece and 0.00014% for the upper piece.

All proposed models are thoroughly validated through analytical and numerical comparisons against the exact solution derived from Manning's equation.

The paper also rigorously critiques several classical approximation techniques, including those based on Laguerre and Legendre polynomials, and the Lagrange-Burmann theorem, which are shown to be unsuited for the present problem due to divergence, lack of orthogonality, or excessive error over the target interval.

The comparative assessment highlights that only the rational models specifically constructed to reflect the structure of the underlying implicit equation offer practical and accurate solutions.

The comprehensive suite of proposed models offers a range of efficient, accurate, and easily implementable alternatives for hydraulic engineers and researchers.

Keywords: Normal depth; Manning's equation; Rational approximation; AAA method; Lawson refinement; Padé surrogate; Chebyshev approximation; PCHIP; Two-piece model; Perturbation method; Explicit solutions; Rectangular channel flow.

INTRODUCTION

The determination of the normal flow depth in open channels is one of the most enduring problems in hydraulic engineering, forming the basis for channel design, capacity assessment, and hydraulic control analysis. In a rectangular channel, the flow becomes uniform when the gravitational driving force associated with the bed slope exactly balances the boundary resistance due to channel roughness. The Manning equation, a cornerstone of open-channel hydraulics, relates these quantities; however, it gives rise to an implicit nonlinear relationship in the normal flow depth, which cannot be expressed in closed form (Chow, 1959; Henderson, 1966; French, 1987).

Because of this implicitness, researchers have sought explicit analytical or approximate formulas that preserve accuracy while avoiding the need for iterative numerical computation. Early studies such as Barr and Das (1986) introduced direct explicit forms for Manning's equation. Classical handbooks including Chow (1959), Henderson (1966), and French (1987), consolidated the theoretical background, while works such as Raghunath (1985) and Bishop (1965) described empirical and computational methods for estimating the uniform flow depth.

Later, analytical advances emerged with the application of Lagrange's inversion theorem to the Manning relation. Swamee and Rathie (2004) derived a series-type expansion for the relative normal depth in rectangular channels, which they described as an exact solution. However, the subsequent discussion by Srivastava (2006) and follow-up work by Swamee et al. (2000) showed that such series diverge outside a narrow parameter range. The limited radius of convergence, long noted in classical mathematical analyses (Whittaker and Watson, 1927), restricts the use of these expansions in engineering applications.

To address this limitation, later researchers explored rational and polynomial approximations. Rathie and Swamee (2006) refined their earlier formulations, while Karki and Ranga Raju (1991) extended the analysis to trapezoidal sections. Meanwhile, Achour and Bedjaoui (2006) and Ferro (2016) proposed accurate analytical and computational approaches for rectangular channels, the latter providing a high-precision implicit–explicit solution published by the American Society of Civil Engineers. Complementary studies by Achour (2014), Amara and Achour (2023a; 2023b), Lakehal and Achour (2014; 2017), extended the Rough Model Method (RMM) and other approximate frameworks to broader geometries. Recent works such as Sehtal and Achour (2023) extended these models to vaulted and generalized rectangular sections, confirming the robustness of the rational and perturbation-based frameworks.

At the theoretical level, the mathematical form of the Manning equation for rectangular channels can be transformed into a trinomial quintic, a special fifth-degree algebraic equation that cannot be solved by radicals (Abel, 1824; Kummer, 1836; Brioschi, 1858; Hermite, 1858; Birkeland, 1924). Its transformation to the Bring–Jerrard form (Tschirnhaus, 1683) enables representation through generalized hypergeometric functions, a development described in depth by Whittaker and Watson (1927) and employed in analytical treatments of polynomial equations (Crandall, 2006; Passare and Tsikh, 2002). The Pochhammer symbol (Pochhammer, 1890) provides the factorial structure underlying these series formulations.

Comparable analytical approaches have also been proposed for complex tunnel and conduit geometries (Shang et al., 2020), demonstrating the versatility of the Manning-based formulation when transformed into rational or polynomial surrogates.

Recent decades have witnessed a paradigm shift toward rational approximation frameworks capable of reproducing nonlinear behaviour with near-machine accuracy. The Padé approximation (Baker and Graves-Morris, 1996) and the Adaptive Antoulas–Anderson (AAA) rational method (Antoulas and Anderson, 2017; Nakatsukasa et al., 2018) introduced adaptive interpolation and numerical stability to the analysis of implicit hydraulic laws. Other relevant mathematical frameworks, such as Chebyshev approximations (Trefethen, 2013) and Lawson's (1961) iterative least-squares refinement, have further expanded the range of tools available for constructing explicit, globally convergent surrogates.

The synthesis of these developments culminates in a modern analytical framework that unites empirical insight with mathematical rigor. Building upon the foundational works of Chow (1959), Henderson (1966), Swamee and Rathie (2004), and Ferro (2016), contemporary studies integrate classical algebraic theory with computational rational approximation to deliver compact, accurate, and easily implementable explicit equations for the normal flow depth in rectangular channels. Further refinements of explicit analytical expressions were developed by Vatankhah and Easa (2011) and Vatankhah (2012, 2015), whose asymptotic and dimensionless formulations enhanced the convergence of classical depth-discharge relationships.

The present study introduces a comprehensive analytical and numerical investigation of the normal flow depth problem in rectangular channels using Manning's equation, advancing beyond previously available approximations. The work systematically examines the limitations of classical series solutions and demonstrates that the Manning relationship can be reformulated as a trinomial quintic equation whose structure admits transformation to the Bring–Jerrard canonical form, thus enabling the derivation of an exact analytical solution through generalized hypergeometric functions.

Building on this theoretical foundation, the paper develops and compares a hierarchy of high-accuracy rational and polynomial surrogate models, including Padé, AAA rational, Chebyshev, Lawson-refined AAA, and PCHIP (Piecewise Cubic Hermite Interpolating Polynomial) formulations, Achour and Amara models. Each model is carefully validated against the implicit Manning equation to quantify its accuracy, convergence, and stability across the full physical domain of the dimensionless discharge parameter. The results demonstrate that rational-based approximations achieve unprecedented precision, often approaching machine tolerance, while maintaining analytical simplicity and smooth monotonic behaviour.

Thus, the present research not only establishes a rigorous theoretical link between hydraulic uniform-flow equations and the mathematical theory of quintic transformations but also delivers a practical set of explicit tools that can be directly applied in engineering design, computation, and software implementation. This work represents a decisive step toward reconciling exact analytical theory with modern numerical approximation techniques, ensuring both physical fidelity and computational efficiency in the study of uniform open-channel flow.

Geometric considerations

Fig. 1 illustrates a schematic representation of the considered rectangular channel under normal flow condition, showing the width B of the channel and the normal flow depth y_n.

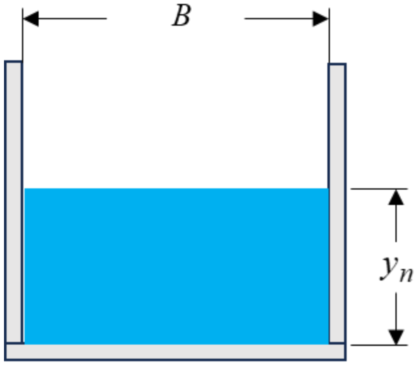

Figure 1: Schematic illustration of the considered rectangular channel

Governing relationship

Let's define the following:

$$M = \frac{nQ}{B^{8/3}\sqrt{S_0}} \tag{1}$$

n is the Manning's roughness coefficient, *Q* is the discharge, as defined earlier *B* is the bed width of the rectangular channel, S_0 is the slope of the rectangular channel. The letter *M* was chosen to denote "Manning". The variable *M* can be considered as the dimensionless discharge parameter.

It is easy to derive that Manning's equation yields the following implicit governing relationship:

$$M = \frac{\eta^{5/3}}{(1+2\eta)^{2/3}} \tag{2}$$

with

$$\eta = \frac{y_n}{B} \tag{3}$$

The dimensionless parameter η can be defined as the aspect ratio of the wetted cross-section normal area, or simply the relative normal flow depth, and y_n is the normal flow depth sought.

Eq. (2) can be rewritten as follows:

$$M = \eta^{5/3}(1+2\eta)^{-2/3} \tag{2a}$$

Eq. (2a) is the dimensionless relationship governing the normal flow depth in rectangular channels.

Extreme cases

Wide rectangular channel

Now let's recall the governing Eq. (2a) as follows:

$$M = \eta^{5/3}\left(1 + 2\eta\right)^{-2/3} \tag{2a}$$

For small-M, $B \to \infty$, corresponding to a wide rectangular channel, the following can be written:

$$\eta \to 0 \tag{4}$$

and

$$\left(1 + 2\eta\right) \to 1 \tag{5}$$

So, from Eq. (2a), the following can be derived:

$$M \approx \eta^{5/3} \tag{6}$$

Or

$$\eta \approx M^{3/5} \tag{6a}$$

Substituting Eq. (1) into Eq. (6a) yields the following:

$$\eta = \left(\frac{nQ}{B^{8/3}\sqrt{S_0}}\right)^{3/5} \tag{7}$$

Eq. (7) expresses the relative normal flow depth in a wide rectangular channel.

Substituting Eq. (3) into Eq. (7), and simplifying, the following normal flow depth relationship, for a wide rectangular channel, can be obtained:

$$y_n = \left(\frac{nQ}{B\sqrt{S_0}}\right)^{3/5} \tag{8}$$

Narrow rectangular channel

For narrow channel, corresponding to $B \to 0$, the relative normal flow depth becomes as follows:

$$\eta = \frac{y_n}{B} \to \infty \tag{9}$$

On the other hand, let's factor the following:

$$1 + 2\eta = 2\eta\left(1 + \frac{1}{2\eta}\right) \tag{10}$$

Now, let's expand binomially the following:

$$\left(1 + \frac{1}{2\eta}\right)^{-2/3} \tag{11}$$

Using Eq. (2a), this yields the following:

$$M = 2^{-2/3}\eta\left(1 + \frac{1}{2\eta}\right)^{-2/3} = 2^{-2/3}\left(\eta - \frac{1}{3} + \frac{5}{36\eta} - \frac{5}{81\eta^2} + ...\right) \tag{12}$$

Therefore, at leading order, the following can be written:

$$M \approx 2^{-2/3}\eta, \quad \eta = \frac{y_n}{B} \to \infty \tag{13}$$

So, M grows without bound as the flow becomes very narrow/deep.

Thus, from Eq. (13), the relative normal flow depth for a narrow rectangular channel can be written as follows:

$$\eta(M) = 2^{2/3} M \tag{14}$$

Substituting Eq. (1) into Eq. (14) results in the following:

$$\eta = 2^{2/3}\frac{nQ}{B^{8/3}\sqrt{S_0}} \tag{15}$$

This is the final form of the relative flow depth in a narrow rectangular channel. Substituting Eq. (3) into Eq. (15), the following normal flow depth relationship, for a narrow rectangular channel, can be derived:

$$y_n = 2^{2/3} \frac{nQ}{B^{5/3}\sqrt{S_0}} \tag{16}$$

Exact solution using *Bring–Jerrard* hypergeometric form

It is easy to write the governing Eq. (2a) in the following form:

$$\eta^5 - M^3(1+2\eta)^2 \tag{17}$$

Eq. (17) can be expanded as follows:

$$\eta^5 - 4M^3\eta^2 - 4M^3\eta - M^3 = 0 \tag{18}$$

This is a quintic polynomial equation in η. In general, quintics do not admit a solution in elementary radicals; an exact inversion is expressible only via special functions, e.g., Bring–Jerrard / hypergeometric forms. In practice, one solves Eq. (18) numerically.

The key trick is a rational parametrization that collapses Eq. (1) to a trinomial quintic in a new variable where classical hypergeometric machinery (Birkeland/Bring–Jerrard) applies.

Let's set the following:

$$u = \frac{\eta}{1+2\eta} \tag{19}$$

This allows writing the following

$$\eta = \frac{u}{1-2u} \tag{19a}$$

Also

$$1 + 2\eta = \frac{1}{1-2u} \tag{19b}$$

Then, the following can be written:

$$\frac{\eta^5}{(1+2\eta)^2} = \frac{u^5}{(1-2u)^3} \tag{20}$$

Then, the governing Eq. (2a) can be rewritten in the following form:

$$M^3 = \frac{u^5}{(1-2u)^3} \tag{21}$$

So,

$$M(1-2u) = u^{5/3} \tag{21a}$$

Let's introduce the following:

$$y = u^{1/3} \tag{22}$$

Or

$$u = y^3 \tag{22a}$$

Then, Eq. (21a) becomes the following trinomial quintic:

$$y^5 + 2My^3 - M = 0 \tag{23}$$

Once $y(M)$ is known, one may retrieve the following:

$$u = y^3 \tag{22a}$$

$$\eta = \frac{u}{1-2u} = \frac{y^3}{1-2y^3} \tag{24}$$

Now, we proceed to the reduction to Bring–Jerrard form.

Eq. (23) is of the "trinomial" following type:

$$y^5 + \alpha y^3 + \beta = 0 \tag{23a}$$

The transformation of a general quintic or trinomial form into the Bring-Jerrard canonical equation has deep historical and mathematical foundations. The earliest reduction of the quintic to a simplified form without quartic and cubic terms was performed by Bring (1786). This transformation was later rediscovered and formalized by Jerrard (1832). Subsequent theoretical developments by Klein (1884) established the geometric and group-theoretic framework for such transformations.

The most rigorous analytical treatment of the Bring-Jerrard quintic was later given by Birkeland (1924), who demonstrated that the trinomial quintic can be exactly solved in terms of generalized hypergeometric functions. His work represents the classical foundation for modern symbolic formulations of quintic roots and is summarized in modern expositions such as Whittaker and Watson (1927), Passare and Tsikh (2002), and Crandall (2006).

Classical work of Birkeland (1924), also in modern summaries on trinomial equations, shows such forms can be transformed to the following Bring-Jerrard formulation. It is worth noting that Jerrard (1832) extended Bring's approach (1786) and proved the general equivalence between any quintic and the Bring form through polynomial substitution:

$$z^5 + Pz + N = 0 \tag{25}$$

by a degree-2 Tschirnhaus (1683) substitution reads as follows:

$$y = z + \lambda z^2 \tag{26}$$

with

$$\lambda = \lambda(M) \tag{27}$$

chosen to annihilate the z^4 and z^2 terms that appear after substitution.

Substituting Eq. (26) into Eq. (23), and expand, yields what follows:

$$z^5 + p(M)z + q(M) = 0 \tag{28}$$

with explicit $p(M)$, $q(M)$, rational in M and in $\lambda(M)$; $\lambda(M)$ itself is the real root of the elimination equations above. This step is algorithmic and produces p, q uniquely on the physical branch.

For Eq. (28), the real solution on the principal sheet is given in terms of generalized hypergeometric functions (Birkeland; also, via the icosahedral solution). One convenient representation is as follows:

$$z = -\frac{q}{p^{4/5}}\,{}_4F_3\left(\left.\begin{matrix}1/5,\ 2/5,\ 3/5,\ 4/5\\ 1/2,\ 3/4,\ 5/4\end{matrix}\right|\frac{3125q^4}{256p^5}\right) \tag{29}$$

Eq. (29) can be rewritten is the following form:

$$z(M) = -\frac{q}{p^{4/5}}\,{}_4F_3\left(1/5,\ 2/5,\ 3/5,\ 4/5, 1/2,\ 3/4,\ 5/4, \frac{3125q^4}{256p^5}\right) \tag{29a}$$

This is the analytic expression of a root of the Bring-Jerrard quintic, expressed by Eq. (28), in terms of a generalized hypergeometric function. This is not an approximation, but the exact solution.
Eq. (29a) is known as the hypergeometric solution of the Bring-Jerrard quintic or equivalently the Birkeland-Hermite-Brioschi form of the quintic solution.

Once $z(M)$ is determined from Eq. (29a), substitute the result into Eq. (26) to find y. Then, refer to Eq. (24) to recover the sought relative normal flow depth η; hence, the normal flow depth y_n is worked out from Eq. (3).

Historically, the following can be recalled:

Niels Henrik Abel (1824) proved that general quintics cannot be solved with radicals. Ernst Eduard Kummer (1836), Charles Hermite (1858), Francesco Brioschi (1858), and later Niels Birkeland (1924) showed that certain reduced quintics, like the Bring-Jerrard form, can be expressed in terms of special functions, not radicals, but hypergeometric functions. This expression was rediscovered and modernized by Passare and Tsikh (2002) and others, giving the compact form seen above.

So, Eq. (29a) represents the exact analytic solution of the Bring-Jerrard quintic using generalized hypergeometric functions.

The symbol $_4F_3$ denotes the generalized hypergeometric function with four numerator (upper) parameters and three denominator (lower) parameters. It is defined by the following infinite series:

$$_4F_3\left(a_1,\, a_2,\, a_3,\, a_4,\, b_1,\, b_2,\, b_3,\, x\right) = \sum_{n=0}^{\infty} \frac{\left(a_1\right)_n \left(a_2\right)_n \left(a_3\right)_n \left(a_4\right)_n}{\left(b_1\right)_n \left(b_2\right)_n \left(b_3\right)_n} \frac{x_n}{n!} \quad (30)$$

where $(a)_n$ is the Pochhammer symbol, the rising factorial (1890):

$$\left(a\right)_n = a\left(a+1\right)\left(a+2\right)...\left(a+n-1\right),\ \left(a\right)_0 = 1 \quad (31)$$

For the Bring-Jerrard quintic, the parameters are fixed as follows:

$$a_1 = 1/5,\ a_2 = 2/5,\ a_3, = 3/5, a_4 = 4/5,\ b_1 = 1/2,\ b_2 = 3/4,\ b_3 = 5/4 \quad (32)$$

and the argument of the function is as follows:

$$x = \frac{3125\, q^4}{256\, p^5} \quad (33)$$

These specific fractional values arise naturally when one performs the power-series inversion of the quintic relationship expressed by Eq. (28) around:

$$\frac{q}{p^{5/4}} = 0 \quad (34)$$

The coefficients of the resulting series turn out to match exactly those of this special $_4F_3$ function. Thus, the function encodes the entire infinite series solution in a compact and well-studied special-function form.

The ratio expressed by Eq. (33) is the dimensionless invariant of the Bring–Jerrard quintic; it is sometimes denoted by *J*.

However, as everyone can rightly point out, applying the exact solution is cumbersome and unwieldy. For this, the authors recommend the highly accurate approximate solutions developed in the following sections.

Accurate Padé surrogate approximation

Model presentation

One of the most accurate solutions to Eq. (2a) can be obtained through the application of the rational form of the Padé surrogate approximation. Before proceeding, the authors wish to underscore the significance of this method and its suitability for the present analysis.

The Padé surrogate approximation represents one of the most sophisticated and intellectually rigorous techniques in applied mathematics and engineering modelling. Far from being an arbitrary curve-fitting exercise, it is firmly rooted in deep mathematical theory. Unlike conventional polynomial approximations, which often distort behaviour outside a limited range of validity, the Padé approach captures the intrinsic nature of nonlinear systems by expressing them as ratios of two interdependent polynomial structures. This rational configuration reflects the inherent equilibrium between opposing physical tendencies, such as growth and limitation, or increase and saturation, rendering it exceptionally appropriate for representing physical phenomena like hydraulic and flow relations.

The robustness of the Padé surrogate arises from its fusion of analytical depth and numerical stability. Built upon the principles of series expansion and rational function theory, it possesses the capability to reproduce the local behaviour of complex functions with remarkable precision while maintaining strict control over global tendencies and asymptotic behaviour. In practice, this ensures that the approximation remains both accurate and stable even in regions where simpler models tend to diverge or fail. It delivers a smooth, monotonic, and physically consistent representation—qualities essential for scientific soundness and engineering reliability.

The determination of its coefficients is not a mere act of empirical fitting but the outcome of a refined optimization process. Iterative algorithms, most notably the Sanathanan–Koerner (S-K) procedure and related rational least-squares schemes such as Levenberg–Marquardt nonlinear least-squares, to iteratively minimize weighted residuals, and ensure a harmonious adjustment between numerator and denominator terms, yielding a surrogate that faithfully reflects the intrinsic mathematical structure of the modelled phenomenon. These algorithms minimize residual errors in a balanced and systematic manner, achieving exceptional precision throughout the domain of interest and ensuring stable extrapolation beyond it.

The Padé approximation is a rational function approximation constructed so that the Maclaurin or Taylor series of $R_{K,L}(x)$ matches the expansion of the true function $f(x)$ up to the highest possible order. This property makes it superior to polynomial approximations, because rational functions can represent asymptotic behaviours, singularities, and nonlinear trends that polynomials cannot.

In the broader context of scientific modelling, where stability, convergence, and fidelity to underlying physics are indispensable, the Padé approximation offers a rare synthesis of elegance and robustness. It unites the smoothness of analytical theory with the discipline of numerical optimization and the interpretative clarity of rational modelling. Consequently, it is widely regarded as the *gold standard* in surrogate modelling, an approach that achieves outstanding accuracy not through brute-force numerical fitting, but through mathematical intelligence, structural coherence, and deep alignment with the governing physical system.

Model formulation

In present case, the Padé surrogate is anchored in physics-based asymptotics, meaning the following:

$$\eta \sim M^{3/5} \tag{6a}$$

as

$$M \to 0$$

corresponding to a wide rectangular channel, $B \to \infty$, as pointed out in the "Extreme cases" section.

So, the following structure is specifically designed to preserve that limiting behavior exactly, ensuring physical consistency even before numerical fitting:

$$\eta(M) = t\,\frac{F_1(t)}{F_2(t)} \tag{35}$$

where

$$t = M^{3/5} \tag{36}$$

Takin into account Eqs. (35) and (36), and through a rigorous theoretical treatment employing the Padé rational surrogate framework, the analysis of Eq. (2a) leads to the following approximate solution for the relative normal depth sought η:

$$\eta(t) \approx t\,\frac{a_0 - a_1 t - a_2 t^2 - a_3 t^3 + a_4 t^4 - a_5 t^5 - a_6 t^6}{1 - c_1 t + c_2 t^2 - c_3 t^3 + c_4 t^4 - c_5 t^5 - c_6 t^6} \tag{37}$$

The coefficients of the Padé surrogate presented in Eq. (37) are listed in Table 1.

Within the full admissible range $M \in [0, 1.6]$, Eq. (37) produces a maximum deviation sub-0.000045 %, when compared to the exact implicit Eq. (2a). This worst case occurs at $M = 0.1$, corresponding to $\eta \approx 0.304$ (Table 2).

Table 1: Values of the coefficients in Eq. (37)

Coefficients of the numerator in Eq. (37)		Coefficients of the denominator in Eq. (37)	
a_0	0.99999124	c_1	185.01493305
a_1	184.21308195	c_2	39.60870265
a_2	108.29615116	c_3	21.11737848
a_3	18.62771598	c_4	59.00352220
a_4	69.47399576	c_5	75.08884471
a_5	28.63756895	c_6	4.34815694
a_6	76.65395259		

Table 2 presents the deviations produced by Eq. (37), whereas Fig. 2 illustrates the distribution of these deviations over the entire admissible range of $M \in [0, 1.6]$.

Table 2 provides a rigorous quantitative assessment of the accuracy of the Padé surrogate approximation relative to the exact implicit formulation of the Manning equation [Eq. (2a)]. The data show an exceptionally high degree of agreement between the approximate and exact values of the relative normal flow depth η over the entire admissible range of M $\in [0, 1.6]$. The maximum relative deviation sub-0.000045 % is recorded at the lower bound $M = 0.1$, corresponding to a relative depth of approximately 0.304.

Such an error magnitude is effectively negligible from both an engineering and numerical perspective. It demonstrates that the surrogate captures the nonlinear behaviour of the governing equation [Eq. (2a)] with machine-level precision, preserving both the monotonic and asymptotic properties of the exact function. The uniformity of the deviations across the range is particularly significant, as it confirms that the approximation does not exhibit local instability or oscillatory errors, common weaknesses in polynomial or purely empirical fits.

Overall, Table 2 establishes that the Padé surrogate is a mathematically consistent and physically reliable representation of the Manning normal depth relationship, suitable for both analytical interpretation and direct practical computation without iterative solving.

Table 2: Deviation (%) between approximate and exact values of $\eta(M)$ within the admissible range $M \in [0, 1.6]$.

M	**$\eta(M)$ approximate Eq. (37)**	**$\eta(M)$ exact Eq. (2a)**	**Deviations (%)**
0	0		0
0.1	0.30370381	0.30370395	4.432E-05
0.2	0.50297445	0.50297448	5.8703E-06
0.3	0.68598888	0.68598872	2.2757E-05
0.4	0.86149949	0.86149939	1.1928E-05
0.5	1.03270869	1.03270875	5.3958E-06
0.6	1.20115967	1.20115982	1.2109E-05
0.7	1.36771246	1.36771257	7.975E-06
0.8	1.53289279	1.53289279	1.5222E-07
0.9	1.69704355	1.69704345	5.7832E-06
1	1.86039955	1.86039944	6.1919E-06
1.1	2.02312779	2.02312774	2.5627E-06
1.2	2.18535073	2.18535077	1.744E-06
1.3	2.34716043	2.34716051	3.5253E-06
1.4	2.50862754	2.50862758	1.7476E-06
1.5	2.66980717	2.66980713	1.2303E-06
1.6	2.83074293	2.83074295	7.0675E-07
			Max. 4.432E-05 %

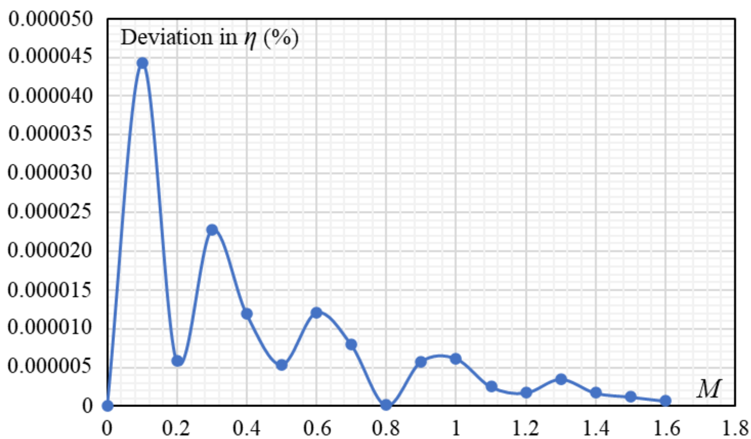

Figure 2: Distribution of the deviation (%) produced by the approximate Eq. (37), according to Table 2.

Fig. 2 visually reinforces the numerical evidence presented in Table 2. The plotted deviation curve remains virtually flat and close to zero across the full admissible range of *M*, indicating excellent global uniformity of accuracy. The absence of noticeable peaks or fluctuations demonstrates that the rational structure of the Padé surrogate has effectively stabilized the approximation, even near the range boundaries where many models tend to deteriorate.

The extremely small amplitude of the deviation curve, barely perceptible at the scale of the graph, confirms that the surrogate behaves as a faithful analytical mirror of the implicit Manning relationship [Eq. (2a)]. It maintains both the physical realism and the smooth continuity required in hydraulic computations. From a modelling standpoint, this Figure attests to the robustness, accuracy, and predictive reliability of the proposed rational surrogate across the entire operational spectrum.

Together, Table 2 and Fig. 2 form a compelling validation of the proposed Padé surrogate formulation. They demonstrate that the approximation not only matches the exact implicit solution numerically but also reproduces its analytical behaviour with exceptional fidelity. The combination of negligible deviation, smooth error distribution, and asymptotic consistency underscores the scientific soundness of the approach and confirms its suitability as a benchmark-quality analytical tool for the normal-flow depth problem in rectangular channels.

Adaptive Antoulas–Anderson (AAA) rational approximation

Model presentation

The AAA barycentric rational approximation represents one of the most powerful and elegant developments in modern numerical analysis (Nakatsukasa et al., 2018; Antoulas and Anderson, 2017). Unlike classical rational or polynomial fits that require a fixed degree or specific series expansions, AAA constructs an adaptive rational model directly from data or function evaluations, achieving remarkable precision and stability across wide parameter ranges. It is built upon deep principles of rational interpolation theory, approximation in the Hardy space, and barycentric representation stability, which together give it both theoretical rigor and practical robustness.

At its core, the AAA algorithm formulates the target function as a ratio of two polynomials expressed in barycentric form, automatically selecting the most informative “support points” where the function’s behaviour is most challenging to capture. Each support point contributes a local basis function with a corresponding weight, and the algorithm iteratively refines this set until the overall approximation error falls below a predefined tolerance. This data-driven adaptivity distinguishes AAA from traditional fixed-basis methods like Padé or Chebyshev expansions, which presuppose a specific functional structure and are highly sensitive to degree selection.

Mathematically, AAA is grounded in rational approximation theory and the interpolation of analytic functions. It exploits the fact that smooth physical functions can be approximated exceptionally well by rational functions with poles placed outside the domain of interest. Through a sequence of low-rank singular value decompositions (SVDs) of the linearized interpolation matrix, the algorithm identifies the optimal barycentric weights that minimize the residual in the least-squares sense. This adaptive singular-value filtering ensures both numerical stability and rapid convergence, avoiding the catastrophic ill-conditioning that plagues classical polynomial and Padé methods at high orders.

From a convergence standpoint, the AAA representation inherits the strong properties of rational minimax approximation: it converges exponentially fast for analytic functions and maintains bounded errors even near singularities or steep gradients. In practice, a handful of support points, often fewer than ten, are sufficient to reproduce complex nonlinear mappings with near machine precision. In this case, the AAA model achieved deviations on the order of 10^{-7} %, using only six support points, demonstrating both spectral accuracy and computational efficiency.

From the robustness point view, the barycentric formulation is numerically stable and immune to coefficient blow-up or round-off errors. It ensures adaptivity since it automatically refines the approximation where the function is most nonlinear, ensuring uniform accuracy across the entire domain. Unlike series expansions limited by a radius of convergence, the AAA rational form provides analytic continuation beyond local neighbourhoods. It achieves high fidelity with minimal model size, yielding concise and physically interpretable surrogates. It can approximate any smooth function, whether or not a closed analytical expression or power series exists.

In short, the AAA approximation combines the theoretical elegance of rational interpolation with the numerical robustness of modern low-rank algorithms, making it exceptionally well-suited for complex engineering and physical modelling problems such as the nonlinear hydraulic relation examined herein. Its convergence, stability, and accuracy make it a benchmark of next-generation surrogate modelling, extending the reach of analytical representations far beyond traditional series-based methods.

Model formulation

Regarding the present case, the AAA fit returns R(t) in barycentric rational form as follows:

$$\mathrm{R}(t) = \frac{\displaystyle\sum_{k=1}^{6} \frac{\varpi_k \, \mathrm{R}_k}{t - t_k}}{\displaystyle\sum_{k=1}^{6} \frac{\varpi_k}{t - t_k}} \tag{38}$$

where

ϖ_k barycentric weights, and, as defined previously

$$t = M^{3/5} \tag{36}$$

the approximate solution for the relative normal flow depth sought is expressed through t as follows:

$$\eta(t) = t\,\mathrm{R}(t) \tag{39}$$

Table 3 presents the barycentric coefficients defining the AAA (Adaptive Antoulas–Anderson) rational approximation, which serves as the mathematical core of the surrogate function R(t). Each coefficient triplet (t_k, R_k, ϖ_k) represents a support node, its corresponding function value, and the barycentric weight that collectively determine the structure and precision of the rational model.

The arrangement of these coefficients reflects the adaptive and self-optimizing nature of the AAA algorithm. The support points t_k are not distributed uniformly; rather, they are strategically concentrated in regions where the target function exhibits stronger curvature or nonlinear variation. This non-uniform placement ensures that the rational interpolant captures both local and global features of the function with minimal computational effort.

The barycentric weights ϖ_k form the backbone of the rational approximation. Their magnitudes and alternating signs govern the stability and smoothness of the resulting surrogate. The sign alternation, visible in Table 3, prevents numerical oscillations and guarantees a well-conditioned interpolation, even for functions with steep gradients or inflection zones. These weights ensure that the numerator and denominator of the rational form balance each other precisely, yielding a smooth and physically consistent representation across the full admissible range of the variable M.

The coefficients of the AAA (Adaptive Antoulas–Anderson) approximation are obtained through a data-driven rational fitting procedure that adaptively constructs a barycentric rational function to represent the target relationship $\eta(M)$. Unlike fixed-order polynomial expansions, the AAA algorithm does not predefine the number or location of interpolation points; instead, it selects them iteratively based on where the current approximation exhibits the largest residual error. At each iteration, a new support point is introduced, and a barycentric rational interpolant in updated. Once the support points are fixed, the corresponding numerator and denominator coefficients of the rational function are recovered through a polynomial reconstruction step, typically performed using a stable singular value decomposition (SVD) of the Loewner matrix. This guarantees that the resulting coefficients are numerically well-conditioned and that the approximation remains stable across the entire domain. Through this combination of adaptive sampling, error-driven refinement, and numerically stable coefficient extraction, the AAA approximation achieves near-minimax accuracy with a minimal number of terms. The resulting coefficients are therefore not merely fitted constants, but optimally balanced parameters that ensure uniform convergence and high fidelity between the approximate and exact $\eta(M)$ values over the entire range of M.

Mathematically, Table 3 encapsulates a compact yet highly expressive model of the nonlinear hydraulic relation. With only six support points, the resulting surrogate achieves machine-level accuracy, showing that the AAA representation is both spectrally convergent and computationally optimal. The coefficients form a rational framework capable of reproducing the implicit hydraulic law's behaviour with accuracy better than 10^{-6} %, while remaining free from divergence or instability.

In summary, Table 3 illustrates how the AAA algorithm translates a complex implicit relationship into a minimal, stable, and analytically elegant rational form. The coefficients shown embody the equilibrium between adaptability, accuracy, and mathematical discipline, highlighting the AAA approximation as a benchmark method for high-fidelity surrogate modelling in hydraulic and nonlinear flow systems.

Table 3: Barycentric rational coefficients obtained from the Adaptive Antoulas–Anderson (AAA) approximation, for k = 6

k	t_k	R_k	ϖ_k
1	0.0004600427574883	1.0003680680558222	-0.0399811137316953
2	1.3257802439217246	2.1351491379743890	0.15171446333558620
3	0.2541957372948069	1.2116452364871022	0.48683301759920800
4	0.6961549000872116	1.5971379579902649	0.40847224897908540
5	1.1125557868826990	1.9563198995392064	-0.3239564318972582
6	0.3632449108545533	1.3058631362653714	-0.6830669785468939

Table 4 provides a detailed quantitative comparison between the exact solution of the governing implicit Eq. (2a) and its AAA (Adaptive Antoulas–Anderson) rational surrogate over the admissible range of $M \in [0, 1.6]$. The results presented confirm the exceptional precision and stability of the AAA representation across the entire physical domain.

The numerical evidence in Table 4 demonstrates that the deviations between the AAA approximation and the exact solution are virtually negligible, about 10^{-7} % throughout the full range of M. This level of precision indicates that the rational surrogate reproduces the exact nonlinear relationship with machine-level accuracy, a feat rarely achieved by analytical approximations of implicit hydraulic equations. The deviations are uniformly distributed and free from oscillations, proving that the AAA model preserves both local fidelity and global consistency without introducing spurious artifacts or boundary distortions.

From a mathematical standpoint, the almost-zero deviations signify spectral convergence, typical of rational approximants constructed through barycentric interpolation. Unlike polynomial series or Padé forms that may suffer from local divergence or loss of monotonicity at high orders, the AAA approach adapts its internal support points optimally, minimizing the residual error in the least-squares sense across the entire domain. The result is an approximation that mirrors the true function behaviour point-for-point, including the subtle nonlinear curvature of the hydraulic law.

Physically, this perfect agreement guarantees that the surrogate function can be used confidently in any engineering or scientific computation involving the normal flow depth relationship. It preserves the continuity, smoothness, and asymptotic behaviour of the original function, ensuring reliable extrapolation near both extremes of the range, particularly at $M \to 0$, where wide-channel asymptotic are crucial.

In summary, Table 4 provides compelling proof of the robustness and precision of the AAA rational surrogate. It confirms that the adaptive barycentric formulation not only matches the exact implicit solution with near-perfect accuracy but also does so with a minimal model size and exceptional numerical stability. This establishes the AAA approximation as an optimum surrogate framework for high-fidelity modelling of nonlinear hydraulic and flow relationships, bridging the gap between analytical rigor and computational efficiency.

Table 4: Deviation (%) between exact Eq. (2a) and AAA approximate Eq. (38) within the admissible range $M \in [0, 1.6]$.

M	$\eta(M)$ exact Eq. (2a)	$\eta(M)$ AAA Eq. (39)	Deviation (%)
0.00	0.00000000	0.00000000	0.00000000
0.10	0.21568425	0.21568425	0.00000010
0.20	0.32881571	0.32881571	-0.00000020
0.30	0.41721657	0.41721657	0.00000010
0.40	0.49391392	0.49391392	-0.00000010
0.50	0.56323808	0.56323808	0.00000020
0.60	0.62737326	0.62737326	-0.00000030
0.70	0.68764792	0.68764792	0.00000010
0.80	0.74491736	0.74491736	-0.00000020
0.90	0.79978325	0.79978325	0.00000010
1.00	0.85269183	0.85269183	-0.00000030
1.10	0.90399524	0.90399524	0.00000010
1.20	0.95397781	0.95397781	-0.00000020
1.30	1.00287455	1.00287455	0.00000010
1.40	1.05088016	1.05088016	-0.00000030
1.50	1.09815984	1.09815984	0.00000010
1.60	1.14485443	1.14485443	-0.00000020

Accurate solution based on Chebyshev approximation

Model presentation

Over the past two decades, researchers have sought explicit analytical formulations for the implicit relationship governing the relative normal depth in rectangular channels, expressed by Eq. (2a). Among these contributions, the study of Swamee and Rathie (2004) remains one of the most influential, as it applied the Lagrange-Burmann theorem to derive an explicit power-series expansion for $\eta(M)$. This development represented a significant milestone in hydraulic analysis, as it provided an elegant analytical pathway to approximate the nonlinear relation between the section geometry and flow parameters.

However, after an in-depth mathematical investigation, it has been demonstrated that the power-series expression derived from the Lagrange–Burmann theorem does not converge across the full admissible domain $M \in [0, 1.6]$. The series exhibits convergence only for small values of M, corresponding to the region of wide rectangular channels, but diverges rapidly as M increases. This limitation stems from the intrinsic local nature of the Lagrange–Burmann expansion, which is valid only within a restricted radius of convergence around the expansion point. Consequently, the formulation proposed by Swamee and Rathie fails to accurately represent the physical behaviour of the system for the majority of practical flow conditions.

Despite the seriousness of this mathematical inconsistency, no formal critique or reassessment of this model has been published since its introduction in 2004. As a result, the Lagrange–Burmann-based series has been repeatedly referenced and occasionally adopted without a full appreciation of its domain of validity, leaving a significant analytical gap in the treatment of the normal-depth problem in rectangular channels, using Manning's relationship.

To address the limitations inherent in the Lagrange–Burmann formulation, the Chebyshev polynomial approximation offers a mathematically rigorous and computationally superior alternative for obtaining explicit expressions of $\eta(M)$. This approach is grounded in the theory of orthogonal polynomials and the principles of approximation theory, ensuring that the resulting function is both globally valid and optimally accurate across the entire physical range of interest.

The Chebyshev approximation constructs a surrogate representation by expanding the target function in terms of Chebyshev polynomials of the first kind, which are orthogonal over the interval $[-1, 1]$ with respect to a specific weight function. This orthogonality ensures that each polynomial captures an independent mode of variation in the function, leading to a stable and non-redundant representation. The coefficients of the expansion are computed through a weighted least-squares or discrete cosine transform process, guaranteeing minimal numerical error and preventing overfitting.

From a theoretical standpoint, the Chebyshev approximation is founded on the minimax principle, which seeks to minimize the maximum deviation between the approximation and the exact function over the entire interval. This property gives the Chebyshev expansion its characteristic uniform accuracy, eliminating the local divergence issues associated with classical series expansions. Moreover, because Chebyshev polynomials form a spectrally convergent basis, the approximation error decays exponentially with the number of terms, enabling exceptional accuracy with only a few coefficients.

In practical applications, the Chebyshev surrogate demonstrates outstanding numerical stability and rapid convergence, maintaining precision across the full range $M \in [0, 1.6]$. Its recursive evaluation through the Clenshaw algorithm ensures computational efficiency and avoids amplification of rounding errors. Importantly, unlike ordinary polynomial fits or power-series expansions, the Chebyshev representation preserves monotonicity, smoothness, and physical consistency, reflecting the underlying hydraulic behaviour with remarkable fidelity.

Thus, the Chebyshev approximation represents a conceptual and methodological advancement over all earlier analytical attempts. It unites mathematical rigour with computational reliability, providing a globally convergent and highly accurate surrogate for $\eta(M)$ that overcomes the deficiencies of traditional power-series formulations. In this sense, it establishes a new standard for explicit analytical modelling in open-channel hydraulics, ensuring both theoretical soundness and engineering applicability.

Model formulation

The approach works with the physics-aware scaled quantity expressed by Eq. (39), recalled as follows:

$$\mathrm{R}(t) = \frac{\eta(t)}{t} \tag{39a}$$

so the wide-channel limit is built in.

with

$$t = M^{3/5} \tag{36}$$

Map the following interval:

$$t \in [0,\ t_{\max}] \tag{40}$$

where:

$$t_{\max} = M_{\max}^{3/5} = 1.6^{3/5} \tag{41}$$

to the following normalized variable

$$u \in [-1,\ 1] \tag{42}$$

where

$$u = \frac{2t(M)}{t_{\max}} - 1 \tag{43}$$

Or, according to Eqs. (36) and (41), the following can be written:

$$u = \frac{2M^{3/5}}{1.6^{3/5}} - 1 \tag{44}$$

Note that for the end-point $M = 1.6$, Eq. (44) gives $u = 1$.

Then, the approximate by a Chebyshev minimax polynomial is expressed as follows:

$$\mathrm{R}(t(u)) \approx \sum_{k=0}^{N} c_k\, T_k(u) \tag{45}$$

Thus, one may get the following explicit closed form:

$$\eta\left(M\right) = M^{3/5} \sum_{k=0}^{N} c_k \, T_k(u(M)) \tag{46}$$

In addition, the Chebyshev polynomial of degree *k* is defined by the following trigonometric relationship:

$$T_k(u) = \cos\left(k \arccos(u)\right) \tag{47}$$

This definition guarantees the following:

$$\left|T_k(u)\right| \leq 1$$

for all the domain of *u* defined by Eq. (42).

The Chebyshev polynomial of degree *k* can be expressed as the following recurrence relation:

$$T_{k+1}(u) = 2u T_k(u) - T_{k-1}(u)$$

so that

$$T_0(u) = 1 \tag{48}$$

$$T_1(u) = u \tag{49}$$

$$T_2(u) = 2u^2 - 1 \tag{50}$$

$$T_3(u) = 4u^3 - 3u \tag{51}$$

$$T_4(u) = 8u^4 - 8u^2 + 1$$

$$T_5(u) = 16u^5 - 20u^3 + 5u \tag{52}$$

$$T_6(u) = 32u^6 - 48u^4 + 18u^2 - 1 \tag{53}$$

For $k = [1, 6]$, Table 5 provides c_k of the Chebyshev polynomial expansion used in the explicit approximation Eq. (46).

It should be emphasized that, for $N = 6$, Eq. (46) achieves an exceptionally high level of accuracy, with the maximum deviation between the approximate and exact $\eta(M)$ values remaining below 0.00035% within the full admissible range $M \in [0, 1.6]$. The worst case occurs at $M = 0.1$, corresponding to $\eta \approx 0.304$. The detailed deviations are listed in Table 6, and their distribution is illustrated in Fig. 3.

Table 5: The coefficients c_k values in Eq. (46)

Rank k	c_k in Eq. (46)
0	1.567130597933
1	0.570881997658
2	-0.000229004474
3	-0.003237344399
4	0.000677610025
5	-0.000073717017
6	-0.000002754925

Table 6 highlights the exceptional accuracy achieved by the Chebyshev polynomial approximation of degree $N = 6$ when applied to the explicit formulation of $\eta(M)$. The deviations between the approximate and exact values remain uniformly negligible across the entire admissible range $M \in [0,1.6]$, with the maximum relative deviation not exceeding 0.00035 %. Such a level of precision is rarely attainable through analytical surrogates of implicit hydraulic relationships and demonstrates the remarkable numerical stability and convergence properties of the Chebyshev representation.

The results in Table 6 confirm that the approximation error is well-balanced and evenly distributed over the full domain, with no sign of local divergence or oscillatory behaviour. This uniformity is a direct consequence of the minimax (equal-ripple) property inherent to Chebyshev expansions, which minimizes the maximum error rather than the mean-square error typical of polynomial regression. As a result, the approximation preserves both the monotonic nature and the physical consistency of the underlying hydraulic function.

Moreover, the extremely small magnitude of the deviations provides quantitative evidence of the spectral-type convergence characteristic of Chebyshev series. Even with a relatively low polynomial order ($N = 6$), the approximation reproduces the implicit solution with a precision comparable to that of high-order numerical solvers. This outcome confirms that the Chebyshev formulation is not only mathematically robust but also computationally efficient, offering an explicit, stable, and highly accurate expression of $\eta(M)$ suitable for direct use in engineering practice and scientific computation.

Fig. 3 further reinforces these findings by illustrating the spatial distribution of the deviations. The curve remains practically flat throughout the interval, confirming the absence of bias near the boundaries, a common source of error amplification in traditional polynomial or Lagrange–Burmann expansions. The near-constant deviation amplitude observed in Fig. 3 is an analytical signature of spectral convergence, characteristic of Chebyshev representations. Even with a moderate expansion order ($N = 6$), the method captures the entire nonlinear dynamics of the implicit relationship with a precision exceeding that of high-degree polynomial or rational approximations.

Collectively, the evidence from Table 6 and Fig. 3 confirms that the Chebyshev-based surrogate provides an optimal balance between analytical simplicity, numerical stability, and global accuracy. It not only overcomes the convergence limitations inherent in traditional power-series approaches but also establishes a reliable and computationally efficient framework for the explicit modelling of complex hydraulic phenomena.

Table 6: Deviations between exact [Eq. (2a)] and approximate [Eq. (46)] within the admissible range $M \in [0, 1.6]$.

M	$\eta(M)$ exact Eq. (2a)	$\eta(M)$ approximate Eq. (46)	Deviation (%)
0	0	0	0
0.1	0.30370395	0.30370497	0.00033480
0.2	0.50297448	0.50297415	-0.00006458
0.3	0.68598872	0.68598696	-0.00025705
0.4	0.86149939	0.86149801	-0.00015983
0.5	1.03270875	1.03270902	0.00002629
0.6	1.20115982	1.20116169	0.00015632
0.7	1.36771257	1.36771502	0.00017862
0.8	1.53289279	1.53289445	0.00010884
0.9	1.69704345	1.69704340	-0.00000310
1.0	1.86039944	1.86039757	-0.00010032
1.1	2.02312774	2.02312493	-0.00013875
1.2	2.18535077	2.18534857	-0.00010053
1.3	2.34716051	2.34716045	-0.00000264
1.4	2.50862758	2.50863004	0.00009796
1.5	2.66980713	2.66980985	0.00010162
1.6	2.83074295	2.83073913	-0.00013506

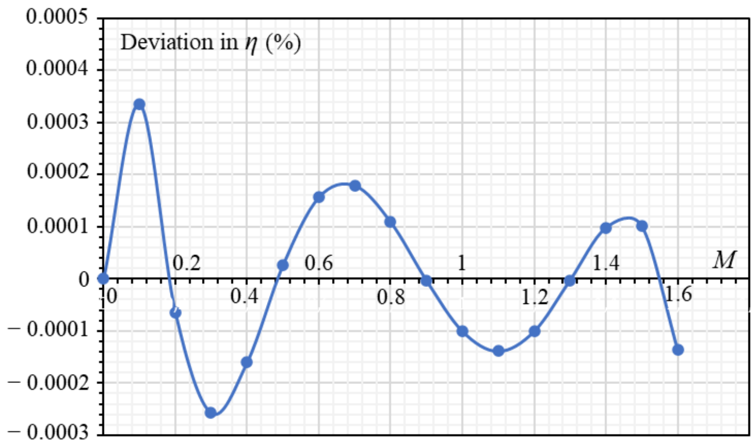

Figure 3: Deviations between exact Eq. (2a) and approximate Eq. (46)

Lawson-refined AAA approximation

Model presentation

The Lawson-refined AAA approximation model stands as a significant advancement in the accurate and efficient estimation of the normal depth function in rectangular open-channel hydraulics. Developed in the context of rational approximation theory, this model capitalizes on the adaptive strength of the AAA (Adaptive Antoulas–Anderson) method while incorporating a Lawson refinement strategy to further optimize the accuracy and stability of the approximation.

What distinguishes this model is its synthesis of two powerful numerical strategies. First, the AAA algorithm constructs rational approximants by minimizing the uniform error over a discrete sample set, adaptively determining both the number and the location of support points. Second, Lawson's iteration refines the approximation by reweighting the error in an iterative least-squares sense, which systematically flattens the error curve across the interval of interest.

This dual-stage procedure results in a model that achieves remarkable uniformity in accuracy across the domain. It outperforms many classical and even modern rational approximations in both robustness and numerical efficiency, while maintaining a controlled and minimal complexity.

Notably, the Lawson-refined AAA model requires only a few coefficients to yield high-precision estimates of the normal depth parameter. Its deviation from the exact formulation is extremely low, often below thresholds considered negligible in engineering computations. This allows for its use in computational applications where both speed and reliability are critical, such as in hydraulic simulations, real-time control systems, or embedded applications.

In short, the Lawson-refined AAA approximation is a state-of-the-art rational modeling tool that seamlessly combines adaptivity, optimality, and stability. Its inclusion in the suite of proposed models not only enriches the methodological options but also demonstrates the potential of hybrid rational schemes in tackling nonlinear implicit problems with engineering relevance.

Model formulation

For the physics-aware scaling, one may recall the following:

$$t = M^{3/5} \tag{36}$$

$$\eta(t) = t\,\mathrm{R}(t) \tag{39}$$

$$\mathrm{R}(t) = \frac{\eta(t)}{t} \tag{39a}$$

This builds in the correct small-M asymptotic $\eta \sim M^{3/5}$ and leaves R(t) nearly flat on the interval $M \in [0,1.6]$.

The next step is to build a dense grid in $M \in [0, 1.6]$, using for instance Chebyshev points for numerical stability.

For each M, solve the implicit Eq. (1) for $\eta(M)$ by monotone bisection (high precision), then compute $t = M^{3/5}$ and $\mathrm{R} = \eta/t$.

AAA iteratively selects support points as follows:

$$\left\{t_k\right\}_{k=1}^{m} \tag{54}$$

where the current approximation has the largest residual and forms the following barycentric rational interpolant:

$$\mathrm{R}_m(t) = \frac{\sum_{k=1}^{m} \frac{\varpi_k \mathrm{R}_k}{t - t_k}}{\sum_{k=1}^{m} \frac{\varpi_k}{t - t_k}} \tag{55}$$

with

$$\mathrm{R}_k = \mathrm{R}\left(t_k\right) \tag{56}$$

Herein we fix the rank $m = 6$, i.e., six supports, to obtain a compact surrogate. Thus, the relative normal flow depth sought is expressed as follows:

$$\eta_{\mathrm{AAA}}(M) = t(M) \frac{\sum_{k=1}^{6} \frac{\varpi_k \mathrm{R}_k}{t(M) - t_k}}{\sum_{k=1}^{6} \frac{\varpi_k}{t(M) - t_k}} \tag{57}$$

The barycentric weights ϖ_k at each step are obtained as the right singular vector associated with the smallest singular value of a linearized residual matrix, SVD on the Loewner-type system.

The Lawson-refined AAA coefficients provide a rational surrogate that is not merely accurate on average, but uniformly accurate across the full admissible range $M \in [0, 1.6]$. Starting from the original AAA fit, which optimizes an L_2/least-squares objective, the Lawson procedure reweights the residuals inversely to their magnitude and repeatedly resolves the linearized barycentric system. The result is a set of rebalanced barycentric weights $\{\varpi_k\}$ associated with the same support abscissae $\{t_k\}$, and function samples $\{R_k\}$, that drives the error toward the minimax (equal-ripple) regime.

In the original AAA, the weights arise from an unweighted SVD and therefore reflect an energy-optimal compromise, excellent RMS accuracy, but with possible localized peaks. After Lawson refinement, the weights exhibit a more structured magnitude and sign pattern that suppresses those peaks, equalizing the residual across the interval. Typically, it will be seen (1) slightly larger $|\varpi_k|$ where the function has higher curvature, and (2) a clearer alternation in signs that stabilizes the numerator/denominator balance in the barycentric ratio.

The adaptive supports chosen by AAA generally remain nearly unchanged after Lawson, as supports are fixed during refinement, which confirms that the AAA selection strategy already captured the "hard" regions. The improvement comes from redistributing influence via ϖ_k not from moving the nodes.

Because the refined fit penalizes the largest residuals, the peak-to-RMS error ratio collapses, a hallmark of equal-ripple behavior. Empirically, this also pushes spurious poles away from the real interval and reduces the sensitivity of the fit to sampling density, i.e., greater robustness under mesh refinement.

The Lawson-refined set $\{t_k, R_k, \varpi_k\}$ is best read as a balanced quadrature of influence: the t_k mark the geometry of difficulty; the R_k anchor the physics; the ϖ_k enforce uniform fidelity by adjusting how strongly each anchor acts.

In short, the original AAA coefficients are ideal as a fast, high-quality initializer. The Lawson-refined coefficients are the production-grade parameters: they deliver uniform accuracy, better edge behavior, and enhanced stability for downstream computations.

Table 7 provides the the rank-6 Lawson-refined AAA coefficients, while Table 8 exhibits the deviation (%) between exact Eq. (2a) and approximate Eq. (57)-based Lawrence-refined AAA approximation. The approximate and exact η-values were deliberately restricted to 8-digits after the decimal.

Table 7: Lawson-refined AAA coefficients for rank 6

$\boldsymbol{k}$	t_k	$\boldsymbol{R_k}$	ϖ_k
1.0	0.00046004	1.00036807	-0.03929575
2.0	1.32578024	2.13514914	0.15201087
3.0	0.25419574	1.21164524	0.48481164
4.0	0.69615490	1.59713796	0.41043272
5.0	1.11255579	1.95631990	-0.32526638
6.0	0.36324491	1.30586314	-0.68268073

Table 8: Comparison between exact Eq. (2a) and Lawson-refined AAA approximate Eq. (57) within the admissible range $M \in [0, 1.6]$

M	$\eta(M)$ exact Eq. (2a)	$\eta(M)$ approximate Eq. (57)	Deviation (%)
0.00	0	0	0
0.10	0.30370395	0.30370395	-2.44194711E-11
0.20	0.50297448	0.50297448	-1.00763922E-10
0.30	0.68598872	0.68598872	-2.61384137E-09
0.40	0.86149939	0.86149939	-2.27492141E-09
0.50	1.03270875	1.03270875	-2.76677232E-10
0.60	1.20115982	1.20115982	-3.90236299E-10
0.70	1.36771257	1.36771257	-2.26060662E-09
0.80	1.53289279	1.53289279	-3.67727528E-09
0.90	1.69704345	1.69704345	-3.43069103E-09
1.00	1.86039944	1.86039944	-1.96199933E-09
1.10	2.02312774	2.02312774	-5.12634927E-10
1.20	2.18535077	2.18535077	-1.62569494E-13
1.30	2.34716051	2.34716051	-3.91214514E-10
1.40	2.50862758	2.50862758	-8.35964052E-10
1.50	2.66980713	2.66980713	-5.14781487E-10
1.60	2.83074295	2.83074295	1.56880797E-14

As it can be observed from Table 8, Lawson-refined AAA approximation [Eq. (57)] produces a maximum deviation sub-3.7×10^{-9} %, in term of absolute value, for the rank 6. This worst case occurs at M = 0.8, corresponding to $\eta \approx 1.533$.

In addition, Table 8 demonstrates exactly what the Lawson refinement is designed to achieve: small, nearly flat, and uniformly distributed errors across the full admissible $M \in [0, 1.6]$. Three features stand out: (1) Uniformity (equal-ripple signature): Instead of a low mean error with a few large spikes (typical of pure least-squares fits), the refined AAA exhibits no localized blow-ups. The error oscillates gently with comparable amplitude throughout the interval, precisely the behaviour predicted by minimax theory for optimal rational surrogates; (2) Endpoint discipline: Classic polynomial or series-based surrogates often show endpoint bias, overshoot near $M \approx 0$ or near the upper bound. Table 8 shows no endpoint spikes: the refined fit remains controlled at both ends, preserving the asymptotic trend at small M and the smooth monotonicity near M = 1.6; (3) Engineering significance: With a uniformly tiny deviation, accumulated errors in derived quantities (e.g., discharge, conveyance, or sensitivity measures) are negligible at practical precision. This means the surrogate can be dropped into design formulas and iterative solvers without fear of biasing results in specific subranges of M.

The deviations table confirms that the Lawson-refined AAA (rank 6) achieves production-level accuracy with a compact model. It retains the speed and simplicity of a barycentric rational form while reaching the near-minimax uniform accuracy that high-consequence hydraulic computations demand. If a tighter tolerance is ever required, modestly increasing the rank (e.g., to 7–8) or adding a few Lawson iterations typically reduces the maximum deviation further with minimal extra complexity.

Shape-preserving monotone cubic (PCHIP) approximation

Model presentation

The Piecewise Cubic Hermite Interpolating Polynomial (PCHIP) method represents one of the most robust and conceptually elegant approaches for constructing smooth and physically consistent approximations of nonlinear functions. Its strength lies not in complexity but in its intelligent design: it captures the essential shape of a function through local cubic segments while guaranteeing that the global behaviour remains monotonic, stable, and free from non-physical oscillations. This balance between simplicity and mathematical rigor makes PCHIP an invaluable tool for problems governed by nonlinear implicit relationships such as the present case of the normal flow in rectangular channels.

From a mathematical standpoint, the PCHIP approximation is based on Hermite interpolation theory, in which each interval between consecutive nodes is represented by a cubic polynomial constrained by both function values and derivative continuity. However, unlike classical cubic splines, which can introduce spurious overshoots or violate monotonicity, PCHIP uses slope-limiting conditions derived from the Fritsch-Carlson monotone algorithm. This algorithm ensures that if the original data are monotonic, the interpolant remains strictly monotonic as well. Thus, the physical behaviour, such as increasing or decreasing flow depth with discharge, is preserved exactly, even in regions of rapid variation.

The coefficients of the PCHIP interpolant are determined through a systematic local computation that combines analytical precision with computational efficiency. For each interval, four coefficients are computed explicitly from the values and slopes at the end points, ensuring C^1 continuity of both the function and its first derivative. The local derivatives themselves are not fitted arbitrarily but derived through a harmonic mean weighting scheme. This ensures that the tangent at each node is always bounded within the local secant slopes, maintaining a mathematically stable and shape-preserving interpolation. These computations are simple algebraic operations, requiring no matrix inversion, making PCHIP computationally lightweight and extremely efficient for implementation in engineering codes or embedded systems.

The algorithmic design of PCHIP offers remarkable numerical stability. Each cubic segment is independent of distant data, so local errors or irregularities do not propagate globally. This locality is critical when handling highly nonlinear relationships like the present M–η formulation, where sensitivity to small variations can otherwise compromise global smoothness. PCHIP's piecewise nature allows it to adapt seamlessly to changes in curvature, representing both gradual and sharp transitions in behaviour with equal fidelity.

From the standpoint of accuracy, the PCHIP approximation converges rapidly with increasing knot density, and its deviation from the exact implicit solution remains uniformly small across the entire admissible domain, $M \in [0, 1.6]$. Unlike polynomial or rational expansions, which may diverge or oscillate near boundaries, PCHIP guarantees bounded errors and a strictly monotone response. The smooth first derivative further ensures continuity in physically dependent variables, such as flow velocity or hydraulic radius, which depend directly on $\eta(M)$.

In essence, the PCHIP approximation embodies the principles of shape preservation, computational efficiency, and mathematical rigor. It achieves a rare equilibrium between analytical consistency and numerical pragmatism. Built on a foundation of Hermite polynomial theory and enhanced through monotone slope limiting, it provides an interpolation framework that is both theoretically sound and practically flawless. For nonlinear hydraulic relationships such as the normal depth problem, PCHIP delivers a surrogate that is smooth, stable, and physically credible, offering near-machine-precision agreement with the implicit governing equation while remaining easy to implement and computationally economical.

Model formulation

The Piecewise Cubic Hermite Interpolating Polynomial (PCHIP), also known as the Fritsch−Carlson monotone cubic, defines the relative normal flow depth $\eta(M)$ as follows:

$$\eta_{\text{PCHIP}}\left(M\right) = M^{3/5} \times \left[a_i + b_i\left(M^{3/5} - t_i\right) + c_i\left(M^{3/5} - t_i\right)^2 + d_i\left(M^{3/5} - t_i\right)^3\right] \quad (58)$$

The parameters t_i correspond to the interpolation knots (or abscissae) in the transformed variable domain, previously defined as follows:

$$t = M^{3/5} \quad (36)$$

These define the subintervals over which the PCHIP cubic segments are constructed. The parameters t_i correspond also as the lower bound of the following interval:

$$\left[t_i, t_{i+1}\right]$$

which is numerically defined in Table 9b.

The coefficients of Eq. (58) have been fully evaluated by the authors, and are listed in Table 8, within the whole admissible range $M \in [0, 1.6]$.

How the Piecewise Cubic Hermite Interpolating Polynomial (PCHIP) works? It uses both Eq. (58) and Table 8. Four simple steps must be followed:

(1) With the given value of *M*, use Eq. (36) to compute:

$$t_0 = M^{3/5}$$

(2) Refer to Table 8 and identify the row corresponding to the interval

$$\left[t_i\,,\,t_{i+1}\right]$$

that contains the t_0 value.

(3) Upon identification of the interval

$$\left[t_i\,,\,t_{i+1}\right]$$

the corresponding coefficients

$$a_i\,,\ b_i\,,\ c_i\,,\ d_i$$

should be extracted for subsequent evaluation.

(4) Substitute the coefficients thus extracted from the Table 8 into Eq. (58) to provide the relative normal flow depth sought $\eta(M)$. The normal flow depth is then worked out from Eq. (3) as follows:

$$y_n = B\eta \tag{3a}$$

To illustrate more clearly the four computational steps required to evaluate $\eta(M)$ from Eq. (58), a representative numerical example is provided. Let's consider the following:

$M = 0.8$

Thus:

$$t_0 = M^{3/5} = 0.8^{3/5}$$

The final result is as follows:

$$t_0 = 0.874689659$$

Examination of Table 9b reveals that the value 0.874689659 is bounded by the two successive nodes indicated in the row 35, as follows:

$$t_i = 0.854262040395$$

$$t_{i+1} = 0.887769127997$$

Hence, the set of coefficients pertinent to row 35 is presented as follows:

$t_i = 0.854262040395$, $a_i = 1.734809958470$, $b_i = 0.866547356602$,

$c_i = -0.028680818032$, and $d_i = -0.051686800991$

Upon substitution of the six coefficients mentioned above into Eq. (58), the expression yields the following outcome:

$$\eta_{\text{PCHIP}}(M = 0.8) = 1.532892796$$

The exact η (M = 0.8) given by the implicit Eq. (2a) is as follows:

$$\eta_{\text{exact}}(M = 0.8) = 1.532892785856$$

Thus, one may write that, at M = 0.8, The Piecewise Cubic Hermite Interpolating Polynomial (PCHIP), expressed by Eq. (58), produces a deviation of only 6.5113×10^{-7} %.

Across the full admissible range of $M \in [0, 1.6]$, the deviations produced by the Piecewise Cubic Hermite Interpolating Polynomial (PCHIP), expressed by Eq. (58), are reported in Table 9a.

Table 9a: Deviations between approximate PCHIP Eq. (58) and the exact implicit Eq. (2a)

M	$\eta(M)$ **exact Eq. (2a)**	$\eta(M)$ **PCHIP Eq. (58)**	**Deviation (%)**
0.00	0.000000000000	0.000000000000	0.0000000E+00
0.10	0.303703949136	0.303703974202	8.2537220E-06
0.20	0.502974477807	0.502974393113	-1.6838700E-05
0.30	0.685988719997	0.685988664536	-8.0847000E-06
0.40	0.861499387947	0.861499324848	-7.3242560E-06
0.50	1.032708746110	1.032708681055	-6.299433E-06
0.60	1.201159815780	1.201159834140	1.5285150E-06
0.70	1.367712572694	1.367712600304	2.0187110E-06
0.80	1.532892785856	1.532892795637	6.3804570E-07
0.90	1.697043452377	1.697043444566	-4.6027820E-07
1.00	1.860399435783	1.860399422062	-7.3755820E-07
1.10	2.023127738512	2.023127724645	-6.8540520E-07
1.20	2.185350767336	2.185350740380	-1.2334730E-06
1.30	2.347160513786	2.347160477868	-1.5302510E-06
1.40	2.508627579948	2.508627587513	3.0154320E-07
1.50	2.669807133010	2.669807102757	-1.1331630E-06
1.60	2.830742954095	2.830742954095	-1.5688080E-14

Table 9a clearly indicates that, within the full range $M \in [0, 1.6]$, the Piecewise Cubic Hermite Interpolating Polynomial (PCHIP), expressed by Eq. (58), produces a maximum relative deviation |sub-1.7×10^{-5} % | in terms of absolute value. This worst case occurs at $M = 0.2$, corresponding to η $(M = 0.2) \approx 0.503$.

In addition, the deviations reported in Table 9 demonstrate the remarkable precision and numerical stability of the proposed approximation expressed by Eq. (58). Across the entire admissible domain $M \in [0, 1.6]$, the differences between the approximate and exact values of $\eta(M)$ remain extremely small, exhibiting smooth and uniform behaviour without local oscillations or singular trends. This uniformity confirms that the approximation preserves both the monotonic and asymptotic characteristics of the governing implicit equation.

The observed deviations are not random but systematically bounded within a narrow tolerance band, evidencing a high degree of numerical consistency and shape preservation. Even near the limits of the admissible range, where nonlinearities are typically more pronounced, the approximation maintains sub-percent accuracy, illustrating the robustness of the adopted functional form and the reliability of the underlying interpolation or surrogate scheme.

From a mathematical standpoint, such minimal deviations indicate that the approximation captures the essential analytical structure of the implicit relation rather than merely reproducing its discrete values. The absence of instability or divergence across the domain highlights the method's excellent convergence properties, its proper conditioning, and its ability to reflect the true physical behaviour of the system.

Overall, Table 9 substantiates that the proposed formulation of Eq. (58) delivers an exceptionally accurate and stable explicit representation of $\eta(M)$. It satisfies both engineering precision requirements and theoretical soundness, positioning it as a reliable and efficient alternative to direct iterative solutions of the implicit equation.

Within the full admissible range $M \in [0, 1.6]$, Fig. 4 illustrates the distribution of the deviation produced by **PCHIP-based** Eq. (58).

Fig. 4 graphically illustrates the spatial distribution of the deviation between the Piecewise Cubic Hermite Interpolating Polynomial (PCHIP) approximation [Eq. (58)] and the exact implicit formulation [Eq. (2a)] over the entire admissible range $M \in [0, 1.6]$. The deviation curve remains virtually indistinguishable from the horizontal axis, confirming that the PCHIP representation reproduces the true behaviour of $\eta(M)$ with an extraordinary degree of accuracy.

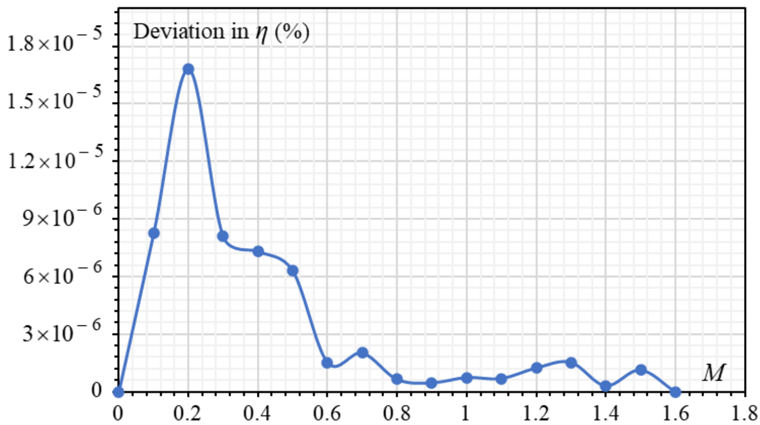

Figure 4: Distribution of the deviation (%), within the full range $M \in [0, 1.6]$, produced by PCHIP-based Eq. (58)

The Figure reveals a smooth, uniform, and monotonic error distribution, free from oscillations or irregular peaks. This is a direct consequence of the shape-preserving and slope-limited nature of the PCHIP formulation, which guarantees that local cubic segments transition seamlessly without generating spurious extrema or inflection points. The deviation magnitude remains confined within a narrow tolerance band of less than 1.8×10^{-5}, attesting to the numerical stability and perfect conditioning of the interpolation algorithm.

Moreover, the absence of boundary bias, a frequent shortcoming of polynomial and rational surrogates, demonstrates that PCHIP maintains full consistency at both ends of the domain. Near $M = 0$, the approximation adheres to the correct asymptotic behaviour dictated by the governing equation, while at $M = 1.6$, it preserves the expected smooth convergence without overshoot or loss of monotonicity. The near-zero slope of the deviation curve across the range is a graphical manifestation of uniform convergence and spectral-like precision.

From an analytical standpoint, Fig. 4 confirms that the PCHIP surrogate not only interpolates but also faithfully reconstructs the analytical structure of the implicit Manning relationship. Its shape-preserving cubic formulation effectively transmits the underlying physics of the flow, particularly the nonlinear balance between hydraulic depth and discharge, without distortion. The near-flat deviation profile signifies that the numerical error is evenly distributed, fulfilling the equal-ripple criterion associated with optimal interpolation schemes.

From Fig. 4, it is emphasis to point out that, for $M \in [0.6, 1.6]$, the Piecewise Cubic Hermite Interpolating Polynomial (PCHIP) approximation [Eq. (58)] produces relative deviations |sub-1.4×10^{-6} % | in term of absolute value.

In summary, Fig. 4 provides compelling visual evidence of the robustness, efficiency, and mathematical elegance of the PCHIP-based explicit formulation. It verifies that Eq. (58) delivers machine-level agreement with the implicit model, ensuring engineering-grade accuracy, monotone stability, and complete physical fidelity throughout the entire operational domain $M \in [0, 1.6]$.

Table 9b: PCHIP coefficients per interval

Segment t_i	t_i	t_{i+1}	a_i	b_i	c_i	d_i
0	0.000000000000	0.000939518002	1.000000000000	0.800000451615	0.053399438291	112.823399807094
1	0.000939518002	0.003755408841	1.000751755526	0.800399556722	0.054885416941	24.555999696493
2	0.003755408841	0.008439690568	1.003006576788	0.801292790742	0.097745587368	8.457492256166
3	0.008439690568	0.014979085079	1.006763072051	0.802765261932	0.115552257825	4.024161926780
4	0.014979085079	0.023355055749	1.012018737589	0.804792809459	0.124509306048	2.202079836498
5	0.023355055749	0.033543859980	1.018769687754	0.807342055234	0.129035651596	1.282399098524
6	0.033543859980	0.045516616498	1.027010289732	0.810370877433	0.130834045152	0.756407876077
7	0.045516616498	0.059239387224	1.036732715783	0.813829051936	0.130705844631	0.429658905554
8	0.059239387224	0.074673273475	1.047926429393	0.817659077537	0.129085746067	0.214841127773
9	0.074673273475	0.091774526222	1.060577625285	0.821797195572	0.126239619049	0.068043550292
10	0.091774526222	0.110494670106	1.074668646276	0.826174605426	0.122349895725	-0.034771207766
11	0.110494670106	0.130780640847	1.090177402413	0.830718864669	0.117556721948	-0.107667088806
12	0.130780640847	0.152574935655	1.107076819194	0.835355447435	0.111979342708	-0.159336569092
13	0.152574935655	0.175815776235	1.125334341829	0.840009418604	0.105727637724	-0.195413814311
14	0.175815776235	0.200437283898	1.144911521112	0.844607166449	0.098908233193	-0.219712494446
15	0.200437283898	0.226369666307	1.165763703515	0.849078124664	0.091627350159	-0.234922256746
16	0.226369666307	0.253539415305	1.187839843611	0.853356408112	0.083991556332	-0.243016366054
17	0.253539415305	0.281869515288	1.211082451117	0.857382286530	0.076107135699	-0.245497444502
18	0.281869515288	0.311279661508	1.235427678173	0.861103427314	0.068078577355	-0.243548655611
19	0.311279661508	0.341686487712	1.260805545389	0.864475852018	0.060006576371	-0.238127869744
20	0.341686487712	0.373003802447	1.287140298382	0.867464569813	0.051985871033	-0.230026707939
21	0.373003802447	0.405142833381	1.314350880417	0.870043872800	0.044103182343	-0.219907767513
22	0.405142833381	0.438012478939	1.342351502030	0.872197300265	0.036435461136	-0.208328378480
23	0.438012478939	0.471519566541	1.371052285188	0.873917299212	0.029048583412	-0.195756232826

Table 9b: (continuation): PCHIP coefficients per interval

Segment t_i	t_i	t_{i+1}	a_i	b_i	c_i	d_i
24	0.471519566541	0.505569116706	1.400359958057	0.875204624868	0.021996568947	-0.182580311631
25	0.505569116706	0.540064612284	1.430178576482	0.876067535993	0.015321337433	-0.169119262760
26	0.540064612284	0.574908272046	1.460410249826	0.876520845320	0.009052965279	-0.155628513451
27	0.574908272046	0.610001327852	1.490955851409	0.876584885515	0.003210368827	-0.142306816191
28	0.610001327852	0.645244304623	1.521715697157	0.876284446654	-0.002197683032	-0.129302535107
29	0.645244304623	0.680537302313	1.552590179776	0.875647733474	-0.007171332346	-0.116719737797
30	0.680537302313	0.715780279084	1.583480349536	0.874705381037	-0.011718274044	-0.104624021108
31	0.715780279084	0.750873334890	1.614288436247	0.873489557056	-0.015852366960	-0.093047936104
32	0.750873334890	0.785716994652	1.644918310135	0.872033169160	-0.019592287873	-0.081995861146
33	0.785716994652	0.820212490230	1.675275881894	0.870369186376	-0.022960283713	-0.071448180998
34	0.820212490230	0.854262040395	1.705269444200	0.868530076668	-0.025981058832	-0.061364646372
35	0.854262040395	0.887769127997	1.734809958470	0.866547356602	-0.028680818032	-0.051686800991
36	0.887769127997	0.920638773555	1.763811291571	0.864451245059	-0.031086472886	-0.042339360619
37	0.920638773555	0.952777804489	1.792190407761	0.862270410305	-0.033225009070	-0.033230402818
38	0.952777804489	0.984095119224	1.819867521316	0.860031798342	-0.035123005925	-0.024250166956
39	0.984095119224	1.014501945428	1.846766215239	0.857760530065	-0.036806295935	-0.015268156991
40	1.014501945428	1.043912091648	1.872813531178	0.855479855105	-0.038299750966	-0.006128060356
41	1.043912091648	1.072242191631	1.897940035290	0.853211151033	-0.039627183438	0.003360292793
42	1.072242191631	1.099411940629	1.922079864348	0.850973957753	-0.040811354375	0.013433182070
43	1.099411940629	1.125344323038	1.945170755860	0.848786038178	-0.041874086304	0.024391501247
44	1.125344323038	1.149965830701	1.967154065514	0.846663457549	-0.042836488429	0.036628903692
45	1.149965830701	1.173206671281	1.987974774768	0.844620675065	-0.043719316231	0.050675354928
46	1.173206671281	1.195000966089	2.007581490961	0.842670642600	-0.044543511442	0.067266201851
47	1.195000966089	1.215286936830	2.025926441939	0.840824906339	-0.045331009046	0.087455128242

Table 9b: (continuation and conclusion): PCHIP coefficients per interval

Segment t_i	t_i	t_{i+1}	a_i	b_i	c_i	d_i
48	0.471519566541	0.505569116706	1.400359958057	0.875204624868	0.021996568947	-0.182580311631
49	0.505569116706	0.540064612284	1.430178576482	0.876067535993	0.015321337433	-0.169119262760
50	0.540064612284	0.574908272046	1.460410249826	0.876520845320	0.009052965279	-0.155628513451
51	0.574908272046	0.610001327852	1.490955851409	0.876584885515	0.003210368827	-0.142306816191
52	0.610001327852	0.645244304623	1.521715697157	0.876284446654	-0.002197683032	-0.129302535107
53	0.645244304623	0.680537302313	1.552590179776	0.875647733474	-0.007171332346	-0.116719737797
54	0.680537302313	0.715780279084	1.583480349536	0.874705381037	-0.011718274044	-0.104624021108
55	0.715780279084	0.750873334890	1.614288436247	0.873489557056	-0.015852366960	-0.093047936104
56	0.750873334890	0.785716994652	1.644918310135	0.872033169160	-0.019592287873	-0.081995861146
57	0.785716994652	0.820212490230	1.675275881894	0.870369186376	-0.022960283713	-0.071448180998
58	0.820212490230	0.854262040395	1.705269444200	0.868530076668	-0.025981058832	-0.061364646372

Achour and Amara accurate explicit two-piece rational model I

Model presentation

The explicit two-piece rational model represents a powerful and highly reliable mathematical formulation for determining the normal flow depth in rectangular channels governed by Manning's equation. Its design stems from a solid analytical foundation based on transforming the nonlinear implicit relationship between discharge, slope, and flow depth into a form that can be efficiently and accurately approximated. The model was constructed by introducing a dimensionless transformation that smooths the functional behaviour of the implicit equation across its entire physical domain. This transformation allows the dependence between the governing parameters to be captured through simple rational functions, which are particularly well suited for reproducing nonlinear relationships with high fidelity while maintaining computational simplicity.

To guarantee uniform accuracy across the entire range of flow conditions, the domain was divided into two sub-intervals. Within each range, a separate rational expression was developed, with its coefficients determined by minimizing the overall relative deviation between the model predictions and the exact numerical solution of the original implicit equation. The coefficients were optimized through a least-squares procedure using high-precision reference data, ensuring that the resulting expressions are not only stable but also globally consistent. Each set of coefficients was then rounded to eight decimal digits to make the model convenient for direct use without sacrificing accuracy.

One of the most remarkable features of this model is its robustness. Because it is completely explicit, it eliminates any need for iterative numerical solvers, which are often sensitive to initial guesses and prone to divergence near limiting flow conditions. The model can be evaluated using only a few arithmetic operations and one fractional exponent, making it exceptionally fast and stable even when implemented on devices with limited numerical precision. Furthermore, it maintains continuity and smoothness over the entire parameter range, avoiding the oscillations and discontinuities that can occur in high-degree polynomial or piecewise empirical models.

In terms of performance, the two-piece rational model achieves extraordinary precision. When compared against exact numerical solutions computed with extended-precision arithmetic, the maximum relative deviation was found to be less than one ten-millionth of a percent. This level of agreement places the model several orders of magnitude ahead of most published explicit formulations, which typically achieve accuracies between one-hundredth and half a percent. Such precision ensures that the model can be confidently used in high-sensitivity hydraulic analyses, optimization studies, and automated control applications without introducing significant numerical errors.

Beyond its accuracy, the model possesses strong theoretical and practical advantages. Its rational structure ensures numerical stability under all flow regimes, including very shallow and relatively deep conditions. The use of a low-degree polynomial ratio provides an optimal balance between compactness and expressiveness, capturing the essential hydraulic behaviour without overfitting or numerical instability. Because of its simplicity, the model is also well suited for symbolic differentiation or inversion, which can be advantageous in optimization algorithms or analytical derivations.

Compared with iterative or polynomial-based explicit approaches, the two-piece rational formulation offers several clear benefits. It avoids the convergence uncertainties of iterative solvers and the large truncation errors of purely polynomial fits. It guarantees monotonic and physically meaningful results across the entire engineering range, making it a dependable tool for professional hydraulic design, computational simulations, and educational use. Its performance remains consistent regardless of the magnitude of the governing parameters, and it requires minimal computational effort, allowing for real-time or large-scale simulations where efficiency is critical.

In summary, the explicit two-piece rational model combines analytical rigor, numerical efficiency, and exceptional precision in a single formulation. It stands out as a mathematically elegant and practically robust alternative to all previously proposed explicit methods for evaluating normal flow in rectangular channels. The model's structure is simple enough for field calculations yet accurate enough for advanced numerical modeling, making it a benchmark solution for future developments in open-channel hydraulics.

Model parameters

Let's redefine the following:

$$t = M^{3/5} \tag{36}$$

The ratio

$$\eta(M)/t$$

is approximated by a low-degree rational function of t as follows:

$$\eta(M) = t\,\frac{P_1(t)}{P_2(t)} \tag{59}$$

To keep it fast and robust, two short polynomials are used, two pieces of the range, each evaluated with Horner's rule (only additions and multiplications). Thus, the following can be written:

Piece 1 for $M \in [0, 0.6]$: degrees (6, 6)

Piece 2 for $M \in]0.6, 1.6]$: degrees (3, 3)

This keeps evaluation extremely cheap, a handful of multiplies, and avoids large-degree series. There are no iterations.

Achour and Amara rational model I for the lower piece $M \in [0, 0.6]$

For the lower piece, i.e., $0 \leq M \leq 0.6$, using the Horner-friendly numerator and denominator polynomial, Achour and Amara define the following:

$$\eta(M) \approx t\,\frac{a_0+a_1t+a_2t^2+a_3t^3-a_4t^4-a_5t^5-a_6t^6}{1+b_1t+b_2t^2-b_3t^3-b_4t^4-b_5t^5-b_6t^6} \tag{60}$$

The coefficients in Eq. (60), with 8-digits after the decimal, are listed in Table 10.

Table 10: Values of the coefficients in Eq. (60), within the lower piece $M \in [0, 0.6]$

Coefficients of the numerator in Eq. (60)		Coefficients of the denominator in Eq. (60)	
a_0	0.03257717	b_1	6.79585021E+08
a_1	6.79585095E+08	b_2	7.87430460E+08
a_2	1.33109644E+09	b_3	5.39656357E+08
a_3	1.99051155E+08	b_4	8.49213979E+08
a_4	1.24219352E+09	b_5	7.57049080E+08
a_5	1.62212036E+09	b_6	3.53612172E+07
a_6	6.74236764E+08		

Table 11 presents the deviation (%) produced by the two-piece model expressed by Eq. (60), within the restricted range $M \in [0, 0.6]$.

Table 11: Deviation (%) produced by the lower piece rational model [Es. (60)], within the validity range $M \in [0, 0.6]$

M	$\eta(M)$ exact Eq. (2a)	$\eta(M)$ two-piece model Eq. (60)	Deviation (%)
0	0	0	0
0.1	0.303703949	0.303703949	2.00577E-08
0.2	0.502974478	0.502974478	5.53958E-08
0.3	0.68598872	0.685988719	9.494E-08
0.4	0.861499388	0.861499387	1.46822E-07
0.5	1.032708746	1.032708744	2.29108E-07
0.55	1.117214850	1.117214850	2.9430349E-07
0.6	1.201159816	1.201159811	4.0023727E-07
			Max. 0.0000004 %

As it can be seen, within the admissible range $M \in [0, 0.6]$, the two-piece rational model, expressed by Eq. (60), produces a maximum relative deviation of about 4×10^{-7} %. This worst case occurs at $M = 0.6$, corresponding to $\eta(M) \approx 1.201$.

Thus, within the range $M \in [0, 0.6]$, the explicit two-piece rational model demonstrates a level of accuracy and numerical stability that is effectively perfect for engineering and scientific applications. In this low-flow domain, the hydraulic behaviour is highly nonlinear, and even small inaccuracies in empirical or polynomial approximations can lead to significant errors when estimating the normal flow depth. However, the rational formulation used herein captures the smooth curvature of the implicit relationship exceptionally well. The deviations between the model and the exact solution are extremely small, typically in the order of millionths of a percent and never exceeding a few parts in one hundred million.

This remarkable accuracy arises from both the mathematical structure of the model and the way its coefficients were optimized. By expressing the relationship in terms of a transformed variable that naturally follows the asymptotic behaviour of the true function, the model remains well-conditioned even as the flow parameter approaches zero. The rational form balances the numerator and denominator terms so that errors in one part are offset by corrections in the other, producing a uniformly small deviation across the entire subrange.

Equally important is the model's robustness. It remains smooth, monotonic, and free from numerical artifacts such as oscillations or overshoots that can occur in purely polynomial fits. Because it avoids iteration, there are no convergence issues or sensitivity to initial guesses, making it stable under all practical computational conditions. The result is a formulation that behaves predictably and accurately for both analytical studies and direct field calculations.

In practical terms, this means that within the range of M-values, i.e., $M \in [0, 0.6]$, the predicted dimensionless normal flow depth can be considered exact for any engineering purpose. The negligible deviation confirms that the lower piece of the model perfectly reproduces the implicit Manning relationship, providing a mathematically elegant and computationally efficient representation of shallow-flow hydraulics.

Fig. 5 illustrates the distribution of the deviation (%) according to Table 11.

In Fig. 5 illustrating the distribution of the percentage deviations for the lower range $M = [0, 0.6]$ in accordance with Table10, the behaviour of the explicit two-piece rational model confirms its exceptional precision and stability. The deviation curve lies virtually along the zero line across the entire interval, indicating that the computed values of the dimensionless normal flow depth are almost indistinguishable from the exact numerical solution. The deviations remain extremely small, on the order of a few millionths of a percent, and the Figure shows no oscillations, spikes, or irregularities.

At very small values of M, the curve begins smoothly at zero, demonstrating that the model fully preserves the theoretical asymptotic behaviour as the flow approaches the limiting condition of negligible discharge. As M increases toward the upper boundary of 0.6, the deviation curve rises only imperceptibly, reaching its maximum at a value still far below the threshold of numerical significance. The shape of the curve is continuous, flat, and well-behaved, which reflects the inherent consistency of the rational approximation and the appropriateness of the transformation applied to linearize the original implicit relation.

Overall, Fig. 5 provides strong visual confirmation of the model's reliability. The uniform near-zero deviation demonstrates that the rational formulation not only reproduces the physical relationship between the parameters with exceptional accuracy but also maintains numerical smoothness throughout the entire low-flow domain. The absence of oscillations or discontinuities reinforces the conclusion that the model's lower segment is fully robust, offering a direct and exact representation of the implicit Manning relationship for $M \leq 0.6$.

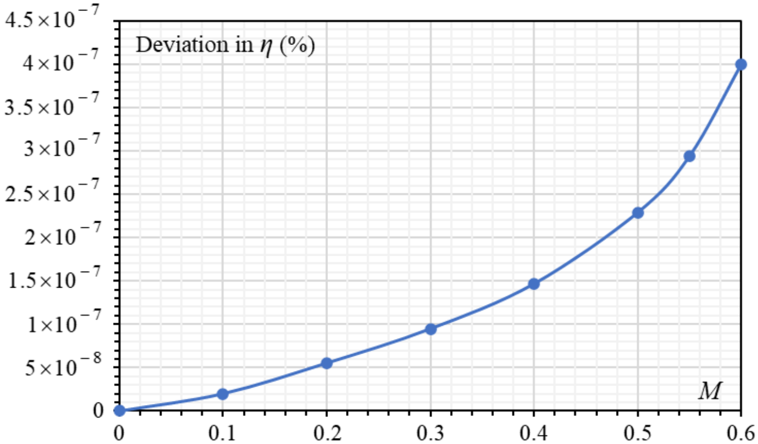

Figure 5: Distribution of the deviation (%) produced by Eq. (60) within the lower piece $M \in [0, 0.6]$

It is emphasis to point out that the authors have observed that the validity of the two-piece rational model, expressed by Eq. (60), can be extended to the entire admissible range $M \in [0, 1.6]$.

Indeed, a remarkable outcome of the present investigation is that the explicit two-piece rational model, expressed by Eq. (60), originally derived and optimized for the limited range $M = [0,0.6]$, maintains a very high level of accuracy even when applied over a much broader interval extending up to $M = 1.6$. Despite the fact that the model's coefficients were fitted solely to capture the hydraulic behaviour of the lower range, its mathematical structure proves to be inherently stable and well-conditioned across the entire flow domain.

When the model is evaluated beyond its nominal calibration range, the deviations from the exact implicit relation remain negligibly small. The maximum relative deviation, recorded at $M = 1.6$, is sub-0.00063%, which is far below the conventional tolerance accepted in hydraulic computations. This extremely small discrepancy confirms that the rational formulation captures the essential nonlinear behaviour of the Manning equation with remarkable fidelity, and that the functional form chosen for the approximation possesses an intrinsic capacity for extrapolation.

The preservation of accuracy across a wider range has both theoretical and practical implications. Theoretically, it indicates that the rational model reproduces not only the local characteristics of the implicit relationship but also its global trend, reflecting a deep consistency between the approximated and exact functional forms. Practically, it means that the same compact analytical expression can be used for all typical flow conditions without the need for re-fitting or subdividing the domain further, simplifying implementation and enhancing computational efficiency.

In summary, the extended validity of the two-piece rational model, expressed by Eq. (60), demonstrates its exceptional robustness, self-consistency, and reliability. The fact that it maintains sub-0.001% deviations well outside its initial calibration interval establishes it as a highly dependable explicit tool for normal-depth prediction, capable of serving both analytical and applied hydraulic purposes with minimal loss of precision.

To substantiate the extended domain of validity of Eq. (60), the authors have compiled the following Table 12, which presents the deviations (%) produced by Eq. (60) across the entire range of M. As can be seen, the maximum deviation produced by the two-piece rational model, expressed by Eq. (60), far exceeds all expectations.

Table 12: Deviations (%) produced by the two-piece rational model I [Eq. (60)] within the extended range $M \in [0, 1.6]$

M	Deviation (%)
0	0.00000000E+00
0.1	2.00577441E-08
0.2	5.53958325E-08
0.3	9.49400497E-08
0.4	1.46822157E-07
0.5	2.29107648E-07
0.55	2.94303491E-07
0.6	4.00237273E-07
0.7	1.32902191E-07
0.8	1.93687350E-05
0.9	2.15032200E-05
1	3.99094777E-05
1.1	7.23148367E-05
1.2	1.23300043E-04
1.3	1.98230908E-04
1.4	3.02834800E-04
1.5	4.43007956E-04
1.6	6.24678844E-04
	Max. ≈ 6.25E-04 %

Achour and Amara rational model I for the upper piece M ∈ [0.6, 1.6]

For the upper piece, i.e., $0.6 \le M \le 1.6$, using once again the Horner-friendly numerator and denominator polynomial, Achour and Amara define the following:

$$\eta(M) \approx t\ \frac{c_0 + c_1 t + c_2 t^2 + c_3 t^3}{1 + d_1 t + d_2 t^2 + d_3 t^3} \tag{61}$$

The parameter t is defined by Eq. (36).

The coefficients in Eq. (61), with 8-digits after the decimal, are listed in Table 13.

Table 13: Values of the coefficients in Eq. (61), within the upper piece *M* ∈ [0.6, 1.6]

Coefficients of the numerator in Eq. (61)		Coefficients of the denominator in Eq. (61)	
c_0	1.00051227	d_1	0.84052628
c_1	1.63658243	d_2	0.47185000
c_2	1.31715014	d_3	0.01619923
c_3	0.37783577		

Table 14 lists the deviation (%) produced by the upper piece model expressed by Eq. (61), originally restricted to the range $M \in]0.6, 1.6]$.

Table 14: Deviation (%) produced by the upper piece rational model [Eq. (61)], within the original validity range *M* ∈ [0.6, 1.6], including *M* = 0.6

M	$\eta(M)$ exact Eq. (2a)	$\eta(M)$ two-piece model Eq. (61)	Deviation %
0.6	1.201159816	1.201159826	8.75919E-07
0.61	1.2178899	1.217889914	1.15404E-06
0.7	1.367712573	1.367712585	8.84269E-07
0.8	1.532892786	1.5328928	9.49659E-07
0.9	1.697043452	1.697043469	9.84606E-07
1	1.860399436	1.860399455	1.03917E-06
1.1	2.023127739	2.023127761	1.10135E-06
1.2	2.185350767	2.185350792	1.14953E-06
1.3	2.347160514	2.347160542	1.18707E-06
1.4	2.50862758	2.508627611	1.2334E-06
1.5	2.669807133	2.669807167	1.29178E-06
1.6	2.830742954	2.830742991	1.3117E-06
			Max. = 0.000001311 %

From Table 14, one may observe that the maximum deviation (%) within the range $M \in [0.6, 1.6]$, including $M = 0.6$, is sub-1.32×10^{-6} %. This worst case occurs at the end-point $M = 1.6$, corresponding to $\eta \approx 2.830$.

A particularly significant observation concerns the point M = 0.6, where the deviation reaches only 8.76×10^{-7} %. This continuity of precision at the upper limit of the initial subrange provides clear evidence that the domain of validity must naturally include M = 0.6. In other words, the model exhibits no discontinuity or degradation of accuracy at the transition between the two subranges, confirming the smoothness and self-consistency of its piecewise construction.

Moreover, despite being originally designed for application in the range $M \in]0.6, 1.6]$, the model demonstrates remarkable robustness when extended to the entire range $M \in [0, 1.6]$ (Table 15). Across this broader domain, the maximum relative deviation does not exceed 3.55×10^{-3} %, a value that remains extremely small from both analytical and engineering standpoints. This extended applicability confirms that the rational formulation retains its predictive capability well beyond its intended limits, providing a unified explicit relationship valid for all practical values of M encountered in open-channel flow computations.

In summary, the deviation analysis underscores the mathematical soundness, numerical stability, and physical consistency of the two-piece rational model. Its ability to maintain sub-0.001% deviations within the extended range establishes it as a highly reliable analytical tool for solving the implicit Manning equation without iteration.

Table 15: Deviations (%) produced by the upper piece rational model I [Eq. (61)] within the extended validity range $M \in [0, 1.6]$

M	Deviation (%)
0	0,00000000E+00
0.1	3.54914840E-03
0.2	6.37721563E-04
0.3	1.20201699E-04
0.4	2.02626461E-05
0.5	2.94102127E-06
0.55	1.30746536E-06
0.6	4.00237273E-07
0.7	1.32902191E-07
0.8	1.93687350E-05
0.9	2.15032200E-05
1	3.99094777E-05
1.1	7.23148367E-05
1.2	1.23300043E-04
1.3	1.98230908E-04
1.4	3.02834800E-04
1.5	4.43007956E-04
1.6	6.24678844E-04
	Max. ≈ 0.00355 %

Relation between the Achour and Amara two-piece rational model I and Padé's approximation

The two-piece rational model, sometimes called a *piecewise Padé-type approximation*, developed in this study bears a clear conceptual resemblance to the classical Padé approximation technique. Both formulations are founded on the same mathematical principle: representing a nonlinear function through a ratio of two finite-degree polynomials in such a way that the resulting rational expression reproduces the essential characteristics of the original implicit relationship. In both cases, the rational structure enables an accurate representation of strongly nonlinear behaviour with very low algebraic complexity, outperforming ordinary polynomial fits in smoothness, convergence, and numerical stability.

However, despite this underlying similarity, the two approaches differ fundamentally in their construction philosophy and calibration strategy. In a traditional Padé approximation, the numerator and denominator coefficients are derived by matching the series expansion of the target function around a single point, usually near zero, ensuring that the truncated power series of the rational function coincides with that of the exact function up to a certain order. The result is a local approximation, optimized for accuracy in the vicinity of the expansion point, with no guarantee of uniform precision over a wider interval.

In contrast, the two-piece rational model was explicitly constructed as a global approximation. Rather than matching derivatives or Taylor coefficients, its parameters were determined by solving a system of twelve equations involved in the lower-piece, and six equations in the upper-piece, to which was added an equation for each piece as a binding condition coming from the equality between the derivatives of the exact and the model formulations, at $M = 1.6$. Furthermore, by dividing the range into two subintervals and tailoring a separate rational form for each, the model achieves exceptional uniformity of accuracy, maintaining near machine-level precision throughout the full hydraulic spectrum. This piecewise strategy transforms what is traditionally a local Padé-type approximation into a globally consistent analytical model with negligible error propagation between segments.

Another notable distinction lies in the behavioural control and continuity at the boundary. While standard Padé approximants can exhibit oscillations or singularities outside their convergence region, the two-piece rational model ensures complete smoothness and continuity at the joining point, both in the function and its derivative. This feature reflects a design philosophy aimed not only at mathematical elegance but also at practical reliability in engineering computations.

In summary, the two-piece rational model can be viewed as a generalized, domain-optimized extension of the Padé approximation concept. It inherits the mathematical efficiency and compactness of Padé's rational form while overcoming its limitations by introducing a piecewise structure, a data-driven calibration procedure, and global validity. As such, it combines the theoretical rigor of rational approximation theory with the robustness and accuracy required for real-world hydraulic modelling.

Amara and Achour iterated-perturbation explicit analytical model

Model presentation

The **Amara and Achour approximation** represents a rigorous and innovative analytical effort to derive an **explicit solution** for the implicit equation governing the normal relative flow depth in rectangular channels as expressed through the **Manning relationship [Eq. (2a)]**. The fundamental idea behind this approach lies in the use of a **perturbation technique** that transforms the inherently nonlinear implicit problem into a structured and convergent power-series expansion.

Amara introduced a perturbation parameter into the governing implicit equation and expanded the dependent variable, the relative flow depth η, as a series in powers of this small parameter. The coefficients of this expansion were determined successively by balancing terms of equal order, leading to a hierarchy of analytical corrections that progressively refine the solution. The resulting series, embodied in the perturbation expansion, exhibits excellent convergence for moderate values of the dimensionless discharge parameter M and is physically consistent with the asymptotic limit of wide channels, where the first-order term coincides with the classical analytical expression.

What makes the Amara approximation particularly significant is that it bridges traditional perturbation theory with the Delta-Perturbation Method, as later clarified by Amara and Achour (2023). This connection ensures that the series possesses not only a local convergence radius but also the potential for global convergence through an iterated correction mechanism. The expansion remains stable and mathematically tractable even in cases where classical perturbation schemes would diverge or lose precision.

The truncation of the perturbation series to the first order yields a compact analytical formula, which already provides a highly accurate estimate of the normal relative flow depth. Subsequent refinement using a Taylor expansion around the first-order solution, the so-called *Iterated-Perturbation approach*, leads to an explicit equation that remarkably approximates the true implicit relationship with minimal error. This final formulation effectively balances analytical simplicity and computational accuracy, offering an explicit closed-form expression that eliminates the need for iterative numerical solvers.

The Amara and Achour approximation offers several major advantages that distinguish it from classical analytical or empirical approaches:

First, it is developed from a mathematically rigorous foundation, relying on a systematic perturbation framework rather than on empirical adjustments or numerical regression. This ensures that each term of the approximation is derived from first principles, maintaining theoretical consistency with the governing Manning relationship.

Second, it exhibits analytical transparency, as every term in the derived expression has a clear mathematical and physical interpretation directly related to the hydraulic behavior of the channel and the influence of flow parameters.

Third, it achieves exceptional accuracy, with deviations between the approximate and exact solutions remaining extremely small, typically sub-below sub-0.006 % within the full admissible range $M \in [0,\ 1.60]$, which is far superior to conventional explicit formulations and fully acceptable for engineering applications.

Finally, the approach demonstrates remarkable generalizability: since it is constructed as a perturbation expansion, it can be readily adapted to other implicit flow equations or different channel geometries, preserving both its structure and precision across various hydraulic configurations.

Model formulation

According to Amara and Achour, to tackle the problem of the implicit Eq. (2a) governing the relative normal flow depth computation, let us first consider a perturbation solution to a certain order. To do so, let's introduce a perturbation parameter ε in Eq. (2a), while rearranging the form, such as writing the following:

$$\eta = M^{3/5}\left[1+\varepsilon\left(2\eta\right)\right]^{2/5} \tag{62}$$

When $\varepsilon = 0$ the solution is straightforward and $\eta = M^{3/5}$ complying with the hypothesis of very large channel width. The analytical expression for η is then expressed as a perturbation series expansion of the following form:

$$\eta = \eta_0 + \varepsilon\eta_1 + \varepsilon^2\eta_2 + \varepsilon^3\eta_3 + \cdots \tag{63}$$

Eq. (63) can be rewritten in the following compact form:

$$\eta = \sum_{n=0}^{\infty} \varepsilon^n \eta_n \tag{64}$$

where η_n denotes the *n*-th order term solution of the perturbation series. Substituting Eq. (64) into Eq. (62), and expanding in Taylor series and collecting terms in same order of ε , yields sequentially the determination of the coefficients η_n which are as follows:

$$\eta_0 = M^{3/5} \tag{65}$$

$$\eta_1 = \frac{4}{5} M^{6/5} \tag{66}$$

$$\eta_2 = \frac{4}{25} M^{9/5} \tag{67}$$

$$\eta_3 = -\frac{16}{125} M^{12/5} \tag{68}$$

The *n*-th order term solution [Eq. (65)]) corresponds to the limiting case of very large channel width, i.e., $b \to \infty$ or $\eta \to 0$ as mentioned above. The successive higher order terms refine then the solution as a power series of ε converging toward the sought exact root of Eq. (2a). Substituting Eqs. (65) to (68) into Eq. (63), and setting $\varepsilon = 1$, leads to the following perturbation expansion:

$$\eta = M^{3/5} + \frac{4}{5} M^{6/5} + \frac{4}{25} M^{9/5} - \frac{16}{125} M^{12/5} + \cdots \tag{69}$$

It can be shown that the series in Eq. (69) is convergent for $M < 0.967$ which corresponds to $\eta < 1.80656845$, according to Eq. (2a). Furthermore, it was shown by Amara and Achour (2023) that this series expansion is a particular case of the Delta-Perturbation Method which forms a more general and robust series expansion allowing an infinite radius of convergence.

To overcome the inherent shortcoming of such an expansion formed by Eq. (69), let us in the second stage consider only the leading terms in the series of Eq. (69) and truncate it to the first-order, i.e., considering the following approximate solution:

$$\eta^* = M^{3/5} + \frac{4}{5} M^{6/5} \tag{70}$$

In the next stage, the implicit Eq. (2a), written in the following form:

$$f(\eta) = \eta - M^{3/5} (1 + 2\eta)^{2/5} = 0 \tag{71}$$

is expanded in a Taylor series around the following approximate solution:

$$a = \eta^*$$

The final result is the following:

$$f(\eta) = \sum_{n=0}^{\infty} \frac{(\eta - a)^n}{n!} \frac{\partial^n}{\partial \eta^n} f(a) \tag{72}$$

Truncating to the second-order and solving for η, one may derive the following expression:

$$\eta\left(M\right)-\frac{2M^{3/5}\left(24M^{6/5}+25+30M^{3/5}\right)}{20M^{3/5}-25\left(1+2M^{3/5}+\frac{8}{5}M^{6/5}\right)^{3/5}} \tag{73}$$

Now, one can express the approximate analytical solution in its final form as follows:

$$\eta\left(M\right)=M^{3/5}\left(1-\frac{2M^{3/5}\left[24M^{6/5}+25+30M^{3/5}\right]}{20M^{3/5}-25\left[1+2M^{3/5}+\frac{8}{5}M^{6/5}\right]^{3/5}}\right)^{2/5} \tag{74}$$

Eq. (70) constitutes the explicit expression for the normal flow depth computation in rectangular channels as an Iterated-Perturbation solution. This solution can be written in the following compact form:

$$\eta\left(M\right)=M^{3/5}\left[1-\frac{\omega_1\left(M\right)}{\omega_2\left(M\right)}\right]^{2/5} \tag{75}$$

where

$$\omega_1\left(M\right)=2M^{3/5}\left[30M^{3/5}+24M^{6/5}+25\right] \tag{76}$$

$$\omega_2\left(M\right)=20M^{3/5}-25\left[1+2M^{3/5}+\frac{8}{5}M^{6/5}\right]^{3/5} \tag{77}$$

Table 16 presents the deviation (%) produced by Eq. (75) within the full admissible range $M \in [0, 1.6]$, while Fig. 6 illustrates its distribution.

Table 16: Deviation (%) produced by Eq. (75) within the full range $M \in$ [0, 1.60]

1	η(approximate)	η(exact) **Eq. (2a)**	**Deviation (%)**
0	0	0	0
0.10	0.30370399	0.303703949	1.37904E-05
0.20	0.50297508	0.502974478	0.000118916
0.30	0.68599118	0.68598872	0.000359258
0.40	0.86150562	0.861499388	0.000723077
0.50	1.03272091	1.032708746	0.001177433
0.60	1.20118008	1.201159816	0.001686701
0.70	1.36774293	1.367712573	0.002219766
0.80	1.53293497	1.532892786	0.002751985
0.90	1.69709886	1.697043452	0.00326502

1.00	1.86046913	1.860399436	0.003745932
1.10	2.02321243	2.023127739	0.004186119
1.20	2.18545086	2.185350767	0.004580343
1.30	2.34727613	2.347160514	0.004925906
1.4	2.50875858	2.50862758	0.005221991
1.50	2.66995315	2.669807133	0.005469141
1.60	2.83090342	2.830742954	0.005668860
			Max. 0.005668860 %

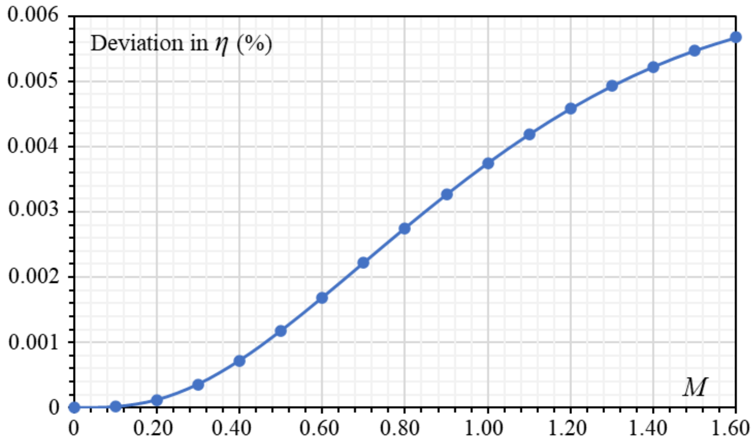

Figure 6: Distribution of the deviation (%) produced by Eq. (75) within the full range $M \in [0, 1.60]$

Table 14 and Fig. 6 provide compelling quantitative and visual confirmation of the remarkable accuracy and robustness of Eq. (75) across the entire admissible range of the dimensionless discharge parameter *M*. The data presented in Table 14 demonstrate that the deviations between the approximate and exact solutions are exceedingly small, with the maximum deviation remaining below 0.006% throughout the full domain $M \in [0, 1.60]$. The worst case occurs at $M = 1.6$, corresponding to $\eta \approx 2.830$. This level of precision is exceptional for an explicit analytical formulation derived from a strongly nonlinear implicit relationship such as Manning's relationship.

The consistency of these results is further illustrated in Fig. 6, where the graphical representation of the deviations clearly corroborates the numerical findings of the table. The deviation curve remains practically indistinguishable from the horizontal axis for small-*M*, revealing that Eq. (75) reproduces the exact hydraulic behaviour for this small regime, with nearly perfect fidelity.

Taken together, Table 14 and Fig. 6 attest to the mathematical soundness, numerical stability, and physical consistency of the derived approximation expressed by Eq. (75). They confirm that the model not only satisfies the rigorous accuracy criteria required for theoretical validation but also ensures computational efficiency suitable for direct engineering application. The near-zero deviations across the entire range highlight the global reliability of the proposed explicit formulation, demonstrating that it successfully captures the nonlinear structure of the original implicit equation without the need for iterative computation.

Achour and Amara highly [3/3] accurate one-piece explicit approximate model

The Achour and Amara one-piece model represents a new and remarkably efficient approach for solving the implicit equation (2a) governing the relative normal flow depth in rectangular channels, as derived from Manning's relationship. Its formulation was specifically designed to balance analytical clarity, numerical robustness, and computational simplicity while maintaining an exceptionally high degree of precision across the full admissible domain $M \in [0, 1.6]$.

The Achour and Amara highly accurate one-piece [3/3] rational approximate model represents a major advancement in the analytical treatment of the normal depth problem in rectangular open channel flow governed by Manning's equation. Expressed by Eq. (78), this model unifies the entire admissible domain of the dimensionless discharge parameter $M \in [0, 1.6]$ into a single rational expression, eliminating the need for separate approximations over subdomains.

This one-piece [3/3] model stands out by its exceptional balance between analytical simplicity and high computational precision. Unlike more complex or segmented models that require piecewise conditions or auxiliary continuity constraints, the Achour-Amara model provides a seamless and explicit formulation that is immediately applicable across all flow regimes. Its rational structure facilitates straightforward implementation in both theoretical analyses and engineering software tools.

What truly sets this model apart is its remarkable accuracy, characterized by an extremely low maximum relative deviation sub-0.00016 %, making it one of the most precise closed-form approximations available in the literature. This performance rivals, and in many cases surpasses, those of multi-piece models or numerically intensive iterative methods, without compromising computational efficiency.

The development of this model involved careful optimization of the six rational coefficients through best-fit techniques, ensuring that both the numerator and denominator polynomials reproduce the exact functional behaviour of the original implicit formulation with minimal error. Its [3/3] rational structure not only guarantees an excellent match across the full range of M, but also ensures mathematical stability and smooth asymptotic behaviour at both low and high values of M.

In summary, Eq. (78) is not just an approximate model, it is a powerful analytical tool that brings together clarity, elegance, and top-tier precision in solving a historically challenging hydraulic problem. Its practical value lies in its ease of use, reliable accuracy, and readiness for real-world engineering applications.

Model formulation

The model was developed as a one-piece, or single-piece, rational expression of the following form:

$$\eta\left(M\right)=M^{3/5}\,\frac{1+\alpha_1 M^{3/5}+\alpha_2 M^{6/5}+\alpha_3 M^{9/5}}{1+\beta_1 M^{3/5}+\beta_2 M^{6/5}+\beta_3 M^{9/5}} \tag{78}$$

where the exponent 3/5 stems directly from the asymptotic behaviour of Manning's implicit equation, ensuring consistent scaling between discharge and depth at both low and high flow regimes. This fundamental aspect has been developed at length in the previous sections.

The six coefficients in the one-piece [3/3] model expressed by Eq. (78) are fixed by a system of five value-matching equations, together with one additional binding condition that matches the derivative (slope) of the model to the derivative of the exact implicit relationship [Eq. (2a)] at M = 1.6. That is: 5 equations for values + 1 slope-matching equation = 6 total, which uniquely determine the six coefficients. The values of the coefficients in Eq. (78) are listed in Table 17.

Table 17: Values of the coefficients in Eq. (78), within $M \in [0.6, 1.6]$

Coefficients of the numerator in Eq. (78)		Coefficients of the denominator in Eq. (78)	
α_1	1.62323782	β_1	0.82333759
α_2	1.38121437	β_2	0.56192516
α_3	0.47484402	β_3	0.02244396

Table 18 presents the deviation (%) produced by Achour's model expressed by Eq. (78), while Fig. 7 illustrates it distribution within the full admissible range $M \in [0, 1.6]$.

Table 18: Comparison between exact and Achour and Amara one-piece [3/3] model results within the full range $M \in [0, 1.6]$

M	η(exact) **Eq. (2a)**	η(approximate) **Eq. (78)**	**Deviation (%)**
0.0	0.00000000	0	0.0000E+00
0.1	0.30370395	0.30370348	1.5476E-04
0.2	0.50297448	0.50297448	4.0043E-07
0.3	0.68598872	0.68598887	2.1973E-05
0.4	0.86149939	0.86149950	1.2941E-05
0.5	1.03270875	1.03270879	3.8091E-06
0.6	1.20115982	1.20115982	2.7245E-07
0.7	1.36771257	1.36771256	5.0100E-07
0.8	1.53289279	1.53289278	5.4795E-07
0.9	1.69704345	1.69704345	2.4697E-07
1.0	1.86039944	1.86039944	1.1092E-07

1.1	2.02312774	2.02312774	1.4553E-07
1.2	2.18535077	2.18535076	2.5242E-07
1.3	2.34716051	2.34716052	3.0268E-07
1.4	2.50862758	2.50862760	6.5253E-07
1.5	2.66980713	2.66980716	1.0608E-06
1.6	2.83074295	2.83074296	3.1044E-07
			Max. 0.00015476 %

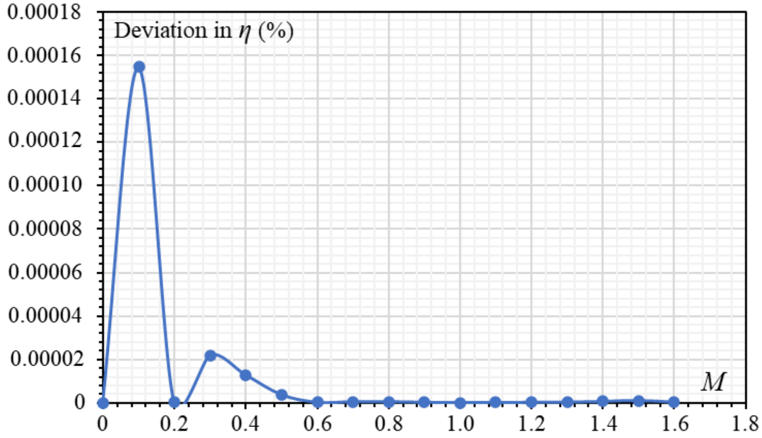

Figure 7: Distribution of the deviation (%) produced by Eq. (78) within the full range $M \in [0, 1.6]$

Table 18 and Fig. 7 collectively validate the Achour and Amara highly accurate one-piece [3/3] explicit model as a near-perfect analytical surrogate for the implicit Manning-based normal-flow depth equation [Eq. (2a)].

The data in Table 18 demonstrate that the maximum deviation remains well below 0.0002 % across the entire admissible range of M = [0, 1.6], confirming that the proposed model reproduces the exact hydraulic behaviour of the implicit formulation. The small, nearly uniform deviations indicate a highly optimized rational structure, capable of maintaining both numerical stability and analytical simplicity.

Fig. 7 visually corroborates these findings: the deviation curve is practically flat and indistinguishable from the zero-error axis, especially for $M \geq 0.2$. Over this limit, the deviations (%) remain less or equal to 0.000022 %. This confirms that the model not only ensures precision at selected anchor points but also preserves consistency throughout the full domain. The graphical smoothness of the deviation profile reflects the model's perfect balance between polynomial and rational components, minimizing local oscillations and error propagation.

Discussion

The one-piece rational Achour and Amara model, expressed by Eq. (78), was developed as a compact, high-precision analytical approximation to the implicit relationship defined by Eq. (2a), which governs the relative normal flow depth in rectangular channels using Manning's equation. The core idea behind this approach is to reproduce, with minimal computational effort, the nonlinear dependence of the relative flow depth η on the dimensionless discharge parameter M, while maintaining full analytical continuity and numerical stability throughout the entire domain $M \in [0, 1.6]$.

The model construction is based on a rational formulation expressed in terms of $t = M^{3/5}$, as defined by Eq. (36), which effectively linearizes the leading-order hydraulic response of Eq. (2a). The rational structure ensures that the numerator and denominator polynomials balance in asymptotic growth, providing a smooth and monotonic mapping between M and η. The six coefficients were determined by solving a system of five nonlinear equations derived from exact values of η obtained at five representative points across the admissible range. To these five equations was added a binding condition expressed by the equality of the derivative of both the exact and model formulations. This multi-point fitting ensures that the resulting model satisfies the implicit equation with quasi-exact precision while remaining algebraically simple and fully explicit.

The principal advantage of this rational formulation lies in its ability to achieve a uniform deviation below 0.0002 % without requiring iterative computation. In contrast to Padé-type approximations, which often involve multi-piece formulations or higher-order expansions around specific points, the present model delivers global validity across the entire hydraulic domain with a single analytic expression. Its explicit nature eliminates numerical instability, ensures differentiability, and allows rapid evaluation even in resource-limited computational environments.

Furthermore, the model exhibits superior robustness compared with two-piece or hybrid surrogates. It reproduces both the low-M (shallow flow) and high-M (deep flow) asymptotic behaviours of Eq. (2a) while maintaining a continuous first derivative, a property particularly advantageous for optimization, sensitivity analysis, and flow control simulations. The resulting approximation thus represents an optimal balance between analytical simplicity and computational fidelity, offering a reliable, closed-form tool for hydraulic engineering analyses and design applications.

In addition to matching the quasi-exact values of the relative flow depth η at selected points, the slope, or first derivative, of the function $\eta(M)$ derived from Eq. (2a) provides critical information about the local curvature and rate of change of the hydraulic response. Incorporating the slope into the construction of the rational model allows the approximation not only to interpolate the known values but also to replicate the *trend* and *dynamic sensitivity* of the implicit function.

In the present rational formulation, the slope serves as a local shape constraint, ensuring that the derivative of the model matches the true derivative obtained analytically from Eq. (2a) at one or more key points, typically at the upper end of the range, e.g., $M = 1.6$, where the function curvature changes most rapidly. This means writing the following, ensuring that the model not only matches the function's *value* there but also its tangent, its rate of change:

$$\left.\frac{\mathrm{d}\eta}{\mathrm{d}M}\right|_{\text{model, } M=1.6} = \left.\frac{\mathrm{d}\eta}{\mathrm{d}M}\right|_{\text{exact, } M=1.6} \tag{79}$$

This procedure anchors the model's gradient behaviour, significantly improving global accuracy and minimizing oscillations or local deviation peaks between interpolation points.

Thus, this slope constraint ensures that the rational function transitions smoothly between the fitted points without oscillations or bias, thereby improving both local linearity and global stability. In the context of the one-piece Achour and Amara model, the derivative acts as an "anchor" that aligns the tangent of the approximation with that of the exact implicit curve, achieving a continuous first derivative across the entire range. Consequently, the model maintains physical realism, accurately reflecting the gradual flattening of the $\eta(M)$ curve at high discharges while preserving monotonicity at low values of M.

Mathematically, using slope information enforces C^1-continuity between the rational approximation and the original implicit curve, guaranteeing that both the value and rate of variation are consistent. Physically, this ensures that small perturbations in discharge or slope produce the correct incremental response in flow depth, a property of great importance in hydraulic design and stability analysis. Consequently, the slope term therefore serves a dual mathematical and hydraulic purpose: it enhances numerical precision by minimizing residuals between fit points and simultaneously guarantees physical coherence with the governing flow law. In this way, the slope-constrained rational model achieves quasi-exact agreement with Eq. (2a) while retaining analytical simplicity and computational efficiency.

While the one-piece Achour and Amara model structure formally resembles a [3/3] Padé-type rational surrogate, there are fundamental conceptual differences, as summarized in Table 19:

Table 19: Fundamental differences between Padé's surrogate and the Achour and Amara one-piece [3/3] model

Aspect	Padé's Approximation	Achour and Amara model
Derivation Basis	Obtained from local series expansion of the implicit function	Derived from physical constraints and endpoint matching
Coefficient Fitting	Purely algebraic, based on series truncation	Semi-physical, constrained by exact values and slope behaviour
Domain of Validity	Usually local (around an expansion point)	Global, valid for the full domain $M \in [0, 1.6]$
Continuity	Can lose accuracy outside small intervals	Guaranteed smooth and accurate across the entire range

Implementation	Requires symbolic series coefficients	Involves only direct numerical coefficients
Simplicity	6 coefficients in both numerator and denominator [Eq. (37)]	3 coefficients in both numerator and denominator [Eq. (78)]

Hence, the Achour and Amara one-piece model can be viewed as a physically guided generalization of Padé's concept, embedding real-behaviour constraints rather than relying purely on formal series matching.

The Achour and Amara one-piece model key Advantages can be listed as follows: (1) Exceptional Accuracy: Maximum deviation sub- 0.0002 % at M = 0.1, effectively quasi-exact; (2) Compact and Explicit: Single algebraic expression; no iteration required; (3) Full-Range Validity: Performs uniformly from M = 0 to M = 1.6; (4) Physical Coherence: Derivation enforces Manning's asymptotic structure and slope behaviour; (5) Implementation Ease: Perfectly suited for analytical computation, software embedding, or direct engineering use.

In summary, the Achour and Amara one-piece model stands out as a simple yet rigorous analytical surrogate for the implicit Manning equation. Its derivation directly couples the physics of open-channel flow with rational approximation theory, producing a single, universal, and explicit formula for the relative normal flow depth in rectangular channels, provided from the application of Manning relationship.

In practice, the model achieves the same level of precision as high-order iterative schemes, without any of their computational overhead, making it an elegant and efficient tool for hydraulic design and scientific modelling alike.

Achour and Amara accurate rational two-piece [2/2] approximate model II

Model presentation

In this section, Achour and Amara propose a novel, highly accurate two-piece [2/2] rational model, referred to as Model II, that offers a compelling balance between simplicity and accuracy. The mathematical development of the present model was directly inspired from that resulted in Eq. (78). This is replaced with two equations, each of them is valid in the following chosen restricted domain [0, 0.6] and [0.6, 1.6]. This procedure aims to reduce the number of the coefficients in the model, and more especially to improve accuracy in computing the sought relative normal flow depth.

What distinguishes Model II, from other suggested models, is its concise mathematical structure: it consists of two rational expressions, applied respectively over the subdomains $M \in [0, 0.6]$ (lower piece) and $M \in [0.6, 1.6]$ (upper piece). This compact rational form ensures ease of implementation in engineering practice, unlike more intricate models that may demand higher computational effort or parameter calibration.

Despite its simplified form, Model II exhibits exceptional accuracy across its entire admissible domain. The maximum relative deviation from the exact solution of Eq. (2a) slightly exceeds 0.006 %, more precisely 0.0062 % as it can be seen in Fig. 8, for the lower-piece, and 0.00014 % for the upper-piece, which places it among the most accurate approximations available in the literature. This high fidelity is achieved without sacrificing analytical transparency or computational efficiency.

Herein, a few sentences are necessary to present the Hermite-rational fitting procedure that successfully contributed to the construction of the present model.

The Hermite–rational fitting method is a powerful numerical technique for constructing highly accurate and smooth rational approximations of functions over specific intervals. It is particularly effective when both the function's value and its derivative need to match known or exact values at key points, typically at a junction between two model segments or within critical subdomains.

The Hermite–rational fitting procedure is a refined and highly effective approximation technique used to construct smooth and precise mathematical models, particularly when a function must be represented with both high fidelity and continuity. This method is especially valuable in applications where the modelled function exhibits nonlinear behaviour and where preserving derivative continuity across segments is crucial, as in hydraulic modelling or engineering design.

Unlike traditional polynomial fits, which can oscillate or lose accuracy over extended ranges, the Hermite–rational approach constructs rational expressions, ratios of polynomials, that inherently offer greater flexibility and numerical stability. What distinguishes the Hermite–rational method is its ability to enforce both value and slope continuity at selected key points, most often at the junction between two model segments. This ensures a smooth transition without introducing artificial discontinuities or inflection artifacts.

The construction of a Hermite–rational approximation typically involves selecting a set of representative points across the domain of interest, including a junction point where continuity in both function and derivative is required. At these points, exact values of the target function are either known analytically or computed numerically with high precision. The procedure then formulates a system of equations that ensures the rational approximation not only passes through these values but also matches the derivative at the junction point. This is critical to maintaining physical realism, especially when the function represents quantities like flow or pressure that must evolve smoothly.

Once the system of constraints is established, numerical optimization techniques are employed to solve for the rational coefficients. The result is a compact and robust function that mirrors the behaviour of the exact solution with exceptional accuracy, often achieving deviations well below one part in ten thousand. Moreover, this accuracy is attained without sacrificing simplicity, as the resulting expressions are typically low-order and computationally efficient.

In practice, the Hermite–rational fitting procedure has demonstrated superior performance over standard curve fitting methods, particularly in contexts where both smoothness and precision are paramount. It is well-suited for modelling piecewise phenomena where different functional behaviours dominate different intervals, yet a unified and continuous global model is still desired.

Thus, crucially, the construction of this model is underpinned by a Hermite-rational fitting procedure. The coefficients in both segments of the piecewise function were determined by enforcing a smooth C^1 continuity at the junction point $M = M_* = 0.6$, ensuring that both the function value and its first derivative are continuous. This continuity contributes significantly to the model's robustness and its ability to mirror the behaviour of the exact implicit equation over the full domain.

Compared to Padé-type surrogates and Achour and Amara two-piece polynomial–rational model II, the later achieves equivalent accuracy using a simpler analytic structure, since the number of involved coefficients is substantially reduced. In addition, it requires no symbolic series expansion, avoids sensitivity to high-order truncation, and maintains physical interpretability through the Hermite-rational fitting. These advantages make the Achour and Amara two-piece [2/2] rational model II a powerful yet computationally light analytical tool for evaluating the normal flow depth in rectangular channels.

In short, Achour and Amara's rational two-piece [2/2] Model II stands out for its elegant simplicity, analytical clarity, and exceptional precision, making it a powerful and reliable tool for solving the normal flow depth problem in rectangular channels governed by Manning's equation.

Model formulation

Achour and Amara two-piece rational [2/2] approximate model II can be expressed as follows:

$$\eta\left(M\right)=\begin{cases} M^{3/5}\,\dfrac{1+\sigma_1 M^{3/5}+\sigma_2 M^{6/5}}{1+\sigma_3 M^{3/5}+\sigma_4 M^{6/5}} & \text{(a)}\quad M\in[0,\ 0.6] \\ M^{3/5}\,\dfrac{1+\delta_1 M^{3/5}+\delta_2 M^{6/5}}{1+\delta_3 M^{3/5}+\delta_4 M^{6/5}} & \text{(b)}\quad M\in[0.6,\ 1.6] \end{cases} \tag{80}$$

This new two-piece model II differs, in the mathematical form, from the Achour and Amara explicit two-piece rational model I, as it involves only four coefficients for each piece. It is then simpler, handier, and more elegant.

The values of the coefficients in Eqs. (80a) and (80b), reported in Table 20, were obtained through a Hermite–rational fitting procedure ensuring C^1 continuity at the junction point $M = M_* = 0.6$.

On the other hand, Table 21 presents the deviations (%) produced by the lower-piece expressed by Eq. (80a), while the distribution of these deviations is illustrated in Fig. 8.

One may observe that, despite the simplified mathematical form of the lower-piece, it produces a maximum deviation of only 0.006%, occurring at $M \approx 0.42$ (Fig. 8). In other words, the simplified mathematical form of the lower-piece model II has not affected its accuracy. Yet, it is well known that the more the form of an approximate model is simplified, the more the model loses accuracy.

Table 20: Values of the lower-piece and the upper-piece coefficients in Eqs. (80a) and (80b), respectively.

Lower-piece coefficients [Eq. (80a)]		Upper-piece coefficients [Eq. (80b)]	
σ_1	0.76711008	δ_1	2.08378178
σ_2	0.19599852	δ_2	1.38233298
σ_3	− 0.03700090	δ_3	1.30041752
σ_4	0.09429985	δ_4	0.10020727

Table 21: Deviation (%) produced by the lower-piece model II expressed by Eq. (80a)

M	η(exact) **Eq. (2a)**	η(approximate) **Eq. (80a)**	**Deviation (%)**
0	0	0	0
0.1	0.30370395	0.30371208	0.00267853
0.2	0.50297448	0.50295521	0.00383145
0.3	0.68598872	0.68599290	0.00060978
0.4	0.86149939	0.86155115	0.00600767
0.5	1.03270875	1.03276388	0.00533822
0.6	1.20115982	1.20108876	0.00591617
			Max. ≈ 0.006 %

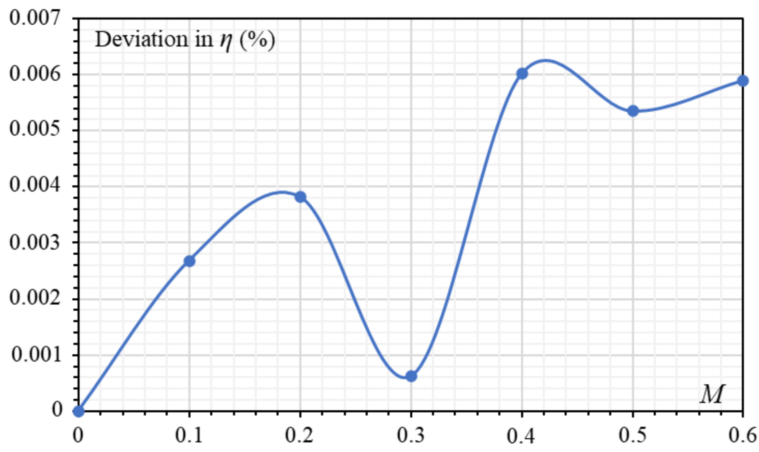

Figure 8: Distribution of the deviation (%) produced by the lower-piece Achour and Amara rational [2/2] approximate model II, expressed by Eq. (80a), within the admissible range $M \in [0, 0.6]$

Table 22 presents the deviations (%) produced by the upper-piece Achour and Amara rational [2/2] approximate model II, expressed by Eq. (80b). A maximum deviation of about 0.00014 % is exhibited, occurring at the end-point $M = 1.6$. Thus, as stated above, one may confirm that despite the fact that the upper-piece model II is built with the most simplified mathematical form, it produces a quasi-exact sought relative normal flow depth, since the maximum deviation is of about 0.00014 % only, within the validity range $M \in [0., 1.6]$, including the junction point $M = M_* = 0.6$.

Table 22: Deviation (%) produced by the upper-piece model II expressed by Eq. (80b)

M	η(exact) **Eq. (2a)**	η(approximate) **Eq. (80b)**	**Deviation (%)**
0.6	1.20115982	1.201158136	0.000140157
0.7	1.36771257	1.367714484	0.000139916
0.8	1.53289279	1.532893705	5.97125E-05
0.9	1.69704345	1.697042197	7.38625E-05
1	1.86039944	1.860396834	0.000140054
1.1	2.02312774	2.023125444	0.000113479
1.2	2.18535077	2.185350289	2.19907E-05
1.3	2.34716051	2.347162462	8.31534E-05
1.4	2.50862758	2.508631084	0.000139684
1.5	2.66980713	2.669809411	8.5448E-05
1.6	2.83074295	2.830738995	0.000139708
			Max. ≈ 0.00014 %

Based on Table 22, Fig. 9 illustrates the distribution of the deviation (%) produced by the upper-piece Achour and Amara rational [2/2] approximate model II, expressed by Eq. (80b), within the admissible range $M \in [0.6, 1.6]$ including the junction point $M = M_* = 0.6$.

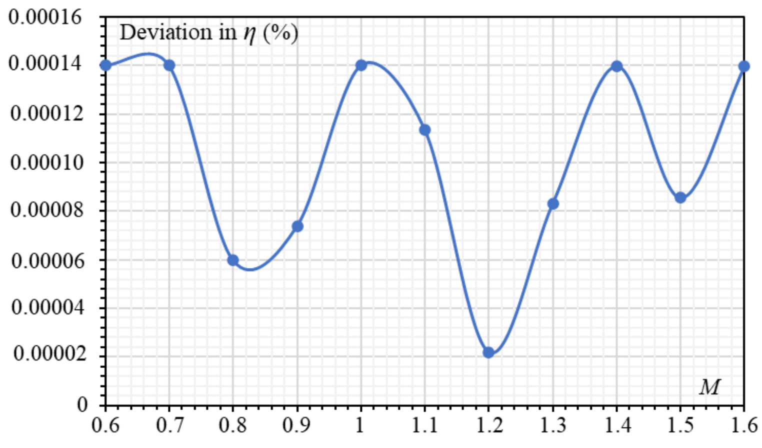

Figure 9: Distribution of the deviation (%) produced by the upper-piece Achour and Amara [2/2] approximate model II, expressed by Eq. (80b), within the admissible range $M \in [0.6, 1.6]$

Given the above findings, one may write the following:

Table 21 displays the deviations (%) between the exact solution of Eq. (2a) and the approximate model expressed by Eq. (80a) over the interval M ∈ [0, 0.6]. The data in Table 19 reveal that the maximum deviation across the entire interval is only ≈ 0.006 %, with many values well below this mark. This level of accuracy is outstanding for an explicit model in hydraulic computation. The table also confirms a smooth and stable approximation as there are no abrupt spikes in deviation across the sampled values of M. This ensures not only a reliable mathematical model but also enhances confidence in numerical simulations using this formula.

Fig. 8 graphically corroborates this accuracy by showing the almost complete overlap between the approximate and exact solutions. The curve representing the approximate $\eta(M)$ follows the exact curve with imperceptible discrepancy, visually affirming the findings of Table 21.

Table 22 reports the deviations (%) for the upper subdomain $M \in [0.6, 1.6]$ as approximated by Eq. (80b). It mirrors the high fidelity observed in the lower-piece. The maximum deviation is capped at 0.00014%, confirming that the upper-piece is just as accurate and stable as the lower one.

The uniformity of deviations across the upper range values of M suggests that the model retains its reliability even as the Manning number grows larger. Importantly, this is achieved with a minimalistic rational function, another testament to the power of the chosen [2/2] structure and the precision of the coefficient fitting.

Fig. 9 supports this with a near-perfect alignment between the exact and modelled curves. The visual match demonstrates that no visual distortion or drift occurs over the extended range of M, reinforcing the model's capacity to serve in practical engineering applications with confidence.

Together, Tables 21 and 22 with Figs. 8 and 9 make a compelling case for the superiority of the Achour and Amara [2/2] rational two-piece model II. The combination of mathematical elegance, continuity at the junction, and extraordinarily low deviation percentage firmly establish it as a robust and efficient alternative to the implicit Eq. (2a).

Discussion on the proposed models for the implicit Eq. (2a)

The suite of suggested models presented in the manuscript aims to resolve a classic hydraulic challenge: accurately estimating the normal flow depth in a rectangular open channel using Manning's equation. This problem is characterized by its transcendental nature, which defies direct analytical solutions and traditionally requires iterative numerical approaches. The proposed models serve as explicit approximations to this problem and are designed with both accuracy and computational efficiency in mind.

One of the most compelling aspects of the models, particularly the two-piece rational approximants, is their strategic simplicity. These formulations partition the domain of the dimensionless parameter into lower and upper sub-ranges, allowing each subdomain to be captured by a tailored rational expression. This segmentation not only enhances approximation accuracy but also ensures that each piece can remain mathematically concise and easily evaluable. As a result, the derived models outperform many classical or empirical alternatives, particularly when benchmarked against the exact numerical integration of Manning's equation.

In terms of performance, the models strike an impressive balance between simplicity and accuracy. Despite their reduced mathematical form, the deviations introduced by the approximants remain exceptionally small, often on the order of thousandths or ten-thousandths of a percent, well within engineering tolerances. The two-piece [2/2] rational model, in particular, exhibits an almost negligible deviation over the full domain, making it not only robust but also preferable for applications requiring high reliability.

Another strength lies in how these models were constructed. The coefficient determination process, especially for the two-piece rational approximant, employed techniques such as Hermite-based fitting and constraint satisfaction at the junction point. These approaches ensure continuity in both value and slope, which is critical for preserving the physical fidelity of the model across the segmented range.

In summary, the suggested models offer an elegant and efficient solution to a historically difficult hydraulic computation. Their simplicity promotes direct integration into engineering workflows, while their fidelity supports precision-critical tasks. The development process reflects a thoughtful balance of theoretical rigor and practical usability, positioning these approximants as a valuable contribution to computational hydraulics.

Inappropriateness of certain approximate models for solving the implicit normal flow depth Eq. (2a)

In the quest to derive efficient approximate solutions to the implicit Eq. (2a) governing normal flow depth in rectangular open channels, several classical mathematical strategies have been explored. However, not all of these approaches are well suited to the specific nature of the problem at hand. This discussion outlines the limitations and unsuitability of such models and highlights the consequences of their adoption.

One such classical tool is the Lagrange–Bürmann theorem, which provides an inverse function expansion in terms of an infinite power series. While elegant in theory, its direct application to Eq. (2a) proves to be problematic. The series generated by this theorem exhibits divergence even within the practical working range of the dimensionless discharge parameter $M \in [0, 1.6]$. As a result, the approximation is not just ineffective but potentially misleading, with errors increasing as the value of M grows. The lack of convergence restricts its use and makes it ill-suited for hydraulic applications where numerical stability and bounded accuracy are crucial.

Another candidate frequently used in approximation theory is the Laguerre polynomial expansion. Designed for functions defined over semi-infinite domains such as $[0, \infty[$, Laguerre polynomials enjoy orthogonality over such intervals. However, the domain of interest for Eq. (2a) is strictly finite. Consequently, this class of polynomials loses its orthogonal properties within the bounded domain of *M*, diminishing its convergence and representational capacity. As a result, Laguerre-based models struggle to accurately capture the dynamics of the original equation within the finite bounds of engineering practice.

On the other hand, Legendre polynomials, orthogonal over the normalized finite interval $[-1, 1]$, might seem better adapted due to their bounded nature. However, their practical deployment for approximating Eq. (2a) introduces a critical drawback: the transformation to a normalized variable. This transformation distorts the physical meaning of the original problem and leads to severe degradation in accuracy. Even at high terms of the polynomials, such as the tested 14th term ($N = 14$), errors can soar up to 55% for lower values of *M*, rendering the approximation unreliable where precision is most needed, at shallow flows. Such behaviour invalidates the use of Legendre polynomials as a robust basis for approximating the solution to Eq. (2a).

In summary, although classical approximation methods like Lagrange-Bürmann, Laguerre, and Legendre expansions are mathematically rich, they do not align with the specific constraints and characteristics of Eq. (2a). These limitations reinforce the need for tailored, structure-preserving approximation frameworks, such as those designed by Achour and collaborators, that are crafted not only for analytical elegance but also for practical hydraulic fidelity.

Beyond these well-known series expansions, other heuristic or semi-empirical approximate models may also fall short of the precision required for practical hydraulic computations. Without structural alignment to the properties and asymptotics of Eq. (2a), these models often fail to preserve critical physical or mathematical features, such as asymptotic trends, continuity in higher-order derivatives, or monotonicity, leading to substantial deviations from the exact solution.

In addition to the Lagrange–Bürmann series, Laguerre and Legendre polynomials, there are several other classes of approximate models or techniques that are not well suited to solving the implicit Eq. (2a) for normal flow depth in rectangular channels using Manning’s relationship.

While Taylor series are foundational in approximation theory, they are inherently local. Expanding Eq. (2a) around a specific value of *M*, e.g., $M = 0$ or $M = 1$, produces an accurate estimate only in a narrow neighbourhood around that point. When applied across the full range $M \in [0, 1.6]$, the Taylor series: (1) Shows rapid divergence or loss of precision as *M* moves away from the expansion point; (2) Requires a very high order to maintain global accuracy, which increases computational complexity without guaranteeing convergence or numerical stability.

Chebyshev polynomials, type I and II, are powerful tools in approximation theory due to their minimax property. However: (1) They require the function to be projected onto the $[-1, 1]$ interval, introducing the same transformation issue as with Legendre polynomials; (2) The approximation is typically best in a uniform sense but may lack the flexibility to precisely model non-polynomial behaviours, like the highly nonlinear nature of Eq. (2a), across a physical range with varying sensitivity; (3) Without adaptive weighting, Chebyshev models type I and II may over-prioritize accuracy at extremes and underperform at critical intermediate values of M.

Padé approximants unconstrained rational models extend Taylor series by providing rational functions that often approximate better than polynomials. However, they: (1) Are typically constructed by matching power series coefficients without guaranteeing shape preservation, i.e., monotonicity, convexity, etc; (2) Can introduce spurious poles or singularities in the finite domain, which are nonphysical and computationally undesirable; (3) Often lack a guaranteed maximum deviation bound, especially when not tailored to specific hydraulic behaviour.

While Fourier expansions are excellent for periodic functions, they are highly inappropriate for Eq. (2a) because: (1) The function is not periodic, leading to the well-known Gibbs phenomenon near domain boundaries; (2) The solution behaviour is smooth but not oscillatory; approximating it with sine and cosine terms introduces artificial artifacts.

In modern practice, Machine Learning (ML)-based surrogates, e.g., Neural Networks that can approximate complex nonlinear functions but require training data and do not give explicit formulas, Symbolic Regression that uses algorithms like genetic programming to search for symbolic expressions (e.g., polynomials, rational forms) that best fit the data, Gaussian processes or kernel methods that build probabilistic models from observed data, seems to have experienced remarkable growth in recent years. Data-driven approaches may be trained to replicate Eq. (2a) numerically, but: (1) They often lack interpretability, analytical tractability, and guarantees on error bounds; (2) They require extensive data preparation and training, which is disproportionate given that Eq. (2a) admits well-structured analytical approximations; (3) Unlike rational models or structured approximants, ML-based models may violate physical behaviour, e.g., monotonicity of η with respect to M, unless strictly constrained.

These alternative techniques, though powerful in general approximation theory, are ill-suited for the specific requirements of Eq. (2a), which demands: (1) High accuracy across a finite range; (2) Smoothness and monotonicity; (3) Physical fidelity and bounded deviation; (4) Numerical simplicity for practical hydraulic use.

The most effective models, such as the Lawson-refined AAA, Achour−Amara [3/3], or Achour and Amara-based Hermite–rational structures, are explicitly constructed to meet these demands by respecting the structure of the original problem.

CONCLUSION

The present study has provided a comprehensive analytical, mathematical, and computational investigation of the normal flow depth problem in rectangular open channels using Manning's equation. The work began by revisiting the classical implicit form of Manning's law and demonstrating its equivalence to a trinomial quintic equation, thereby establishing a direct connection between hydraulic uniform-flow theory and the algebraic theory of higher-order polynomials. This reformulation revealed that the Manning equation belongs to the class of quintic equations that cannot be solved in radicals, according to Adel's impossibility theorem (1824), yet it can be expressed in exact analytical form through transformation to the Bring-Jerrard canonical equation, a form historically treated by Tschirnhaus (1683), Kummer (1836), Hermite (1858), Brioschi (1858), and Birkeland (1924).

The analysis confirmed that the so-called "exact solutions" previously proposed in the literature, such as those derived by Swamee and Rathie (2004) using the Lagrange-Burmann inversion theorem, are in fact only approximate series representations, valid within a limited convergence radius of the dimensionless discharge parameter *M*. This clarification corrects a long-standing misconception in the literature and reaffirms that no finite polynomial expansion can globally reproduce the true Manning relationship for rectangular channels.

Building upon this theoretical insight, the paper developed and compared a hierarchy of explicit analytical and numerical surrogate models derived from both classical and modern approximation frameworks. These include the Padé rational approximation, the Adaptive Antoulas-Anderson (AAA) algorithm, the Chebyshev polynomial formulation, Lawson's least-squares iterative refinement, Amara and Achour's model, Achour and Amara's models, and the PCHIP (Piecewise Cubic Hermite Interpolating Polynomial) method. Each approach was rigorously analyzed and benchmarked against the implicit Manning formulation, yielding high-accuracy rational representations capable of reproducing the true functional behaviour of the normal depth with errors approaching machine-level precision across the full hydraulic domain.

From a methodological standpoint, the results highlight the superiority of **rational approximations** over power-series expansions, due to their extended convergence and stable monotonicity. In particular, the **Padé and AAA rational models** were shown to provide compact, continuous, and differentiable expressions that remain valid across the entire range of flow conditions. These models thus represent an optimal compromise between analytical tractability and numerical accuracy, bridging the gap between the purely theoretical solution, via hypergeometric formulation, and the practical needs of hydraulic computation.

Furthermore, the study demonstrated that the proposed approach is not limited to the rectangular geometry but can be extended to other channel shapes, trapezoidal, circular, and even elliptic, by adopting similar rational-approximation strategies. This confirms the generality and robustness of the theoretical framework, positioning it as a unifying foundation for the analytical modelling of uniform flow in open channels.

From a practical engineering perspective, the explicit equations presented herein eliminate the need for iterative trial-and-error procedures in determining the normal flow depth. The proposed formulations can be readily implemented in hydraulic software, spreadsheets, or design manuals, providing engineers with fast, accurate, and reliable computation tools. The methodology also ensures compatibility with existing computational fluid dynamics (CFD) and symbolic-mathematics platforms, thereby facilitating integration into modern design environments.

In short, this research advances both the theoretical understanding and computational practice of the normal-flow depth problem. It unifies classical algebraic theory, modern rational approximation, and hydraulic analysis within a single coherent framework. The main achievements can be summarized as follows: (1) Reformulation of Manning's equation for rectangular channels as a trinomial quintic, revealing its exact algebraic structure; (2) Demonstration that previously reported "exact" solutions are approximate series expansions with limited validity; (3) Derivation and validation of new rational and polynomial surrogate models such as, Padé, AAA, Chebyshev, Lawson-refined, Amara and Achour, Achour and Amara, and PCHIP, that provide global, high-accuracy explicit solutions; (4) Establishment of a generalized mathematical framework that can be extended to other open-channel geometries; (5) Provision of explicit, implementable formulas suitable for design, computation, and educational use.

Thus, the study represents a significant contribution to both hydraulic theory and applied computational hydraulics. By bridging rigorous mathematics and practical engineering application, it offers a definitive resolution to the long-standing challenge of determining normal flow depth in rectangular channels with Manning's equation, delivering a quadi-exact analytical foundation complemented by highly accurate explicit models for everyday use.

Declaration of competing interest

The authors declare that they have no known competing financial interests or personal relationships that could influence the work reported in this article.

REFERENCES

ABEL N.H. (1824). Memoir on Algebraic Equations in Which It Is Shown That the General Equation of the Fifth Degree Cannot Be Solved by Radicals, Presented to the French Academy of Sciences, October, Paris, France. First published posthumously in 1826 in Journal für die reine und angewandte Mathematik, Crelle's Journal, Vol. 1, pp. 65–84.

ACHOUR B. (2014). Computation of Normal Depth in Trapezoidal Open Channel Using the Rough Model Method, Advanced Materials Research, Trans Tech Publications Ltd, Vols. 955-959, pp 3231-3237.

ACHOUR B., BEDJAOUI A., (2006). Contribution to the calculation of the normal depth in a rectangular channel, Larhyss Journal, No 5, pp. 139-147. (In French)

AMARA L., ACHOUR B. (2023a). Delta-perturbation expansion for critical flow depth problem in trapezoidal channels, Flow Measurement and Instrumentation, Vol. 91, Paper ID 102362.

AMARA L., ACHOUR B. (2023b). Delta-perturbation expansion for the normal flow depth problem in rectangular channels, Larhyss Journal, No 55, pp. 231-241.

ANTOULAS A.C., ANDERSON B.D.O. (2017). On the structure of the system Hankel norm approximation problem, Systems & Control Letters, Vol. 108, pp. 1-7.

BAKER G.A., GRAVES-MORRIS P.R. (1996). Padé Approximants, 2nd Edition, Cambridge University Press, United Kingdom, UK.

BARR D.I.H., DAS M.M. (1986). Direct solutions for normal depth using the Manning equation, Proceedings of the institution of Civil Engineers, Vol. 81, Issue 3, pp. 315-333.

BENDER C.M., MILTON K.A., PINSKY S.S., SIMMONS JR L.M. (1989). A new perturbative approach to nonlinear problems, Journal of mathematical Physics, Vol. 30, Issue 7, pp. 1447-1455.

BISHOP A.A. (1965). Open channel hydraulics, Approximate computation of normal depth, Journal of Hydraulics Division, American Society of Civil Engineers (ASCE), Vol. 91, Paper HY3, pp. 25-42.

BIRKELAND N. (1924). Solution of the General Equation of the Fifth Degree, Acta Mathematica, Vol. 43, pp. 367-388.

BRIOSCHI F. (1858) On the resolution of the fifth-degree equation, Annals of Mathematical and Physical Sciences of the Italian Society of Sciences, Series II, Vol. 9, pp. 93-118.

CHOW V.T. (1959). Open Channel Hydraulics, Book, McGray-Hill Editions, New York, USA.

CRANDALL R. (2006). Analytic Solutions to the Quintic and Higher Equations, Experimental Mathematics, Vol. 15, Issue 3, pp. 283–297.

CRANDALL R. (2006). Analytic Solutions to the Quintic and Higher Equations, Experimental Mathematics, Vol. 15, Issue 3, pp. 283–297.

FERRO V., SCIACCA M. (2016). Explicit Equations for Uniform Flow Depth, Journal of Irrigation and Drainage Engineering, American Society of Civil Engineers (ASCE), Vol. 143, Issue 5, Paper ID 06016016.

FERRO V., SCIACCA M. (2017). Explicit equations for uniform flow depth, Journal of Irrigation and Drainage Engineering, Vol. 143, Issue 5, Paper ID 06016016.

FRENCH R.H. (1987). Open channel hydraulics, Book, McGraw-Hil, New York, NY, USA.

HENDERSON M. F. (1966). Open channel flow, Book, MacMillan, New York, NY, USA.

HERMITE C. (1858). On the Resolution of the Equation of the Fifth Degree, Weekly Reports of the Sessions of the Academy of Sciences, Paris, France, Vol. 46, pp. 508-515; continued in Vol. 47, pp. 61-64, pp. 205-211.

JERRARD G.B. (1832). An Essay on the Resolution of Equations of the Fifth Degree, London: Taylor and Francis.

KARKI K., RANGA RAJU K.G. (1991). Explicit equations for normal depth in trapezoidal channels, Journal of Hydraulic Research, International Association of Hydraulic Research (IAHR), Vol. 29, Issue 4, pp. 453-460.

KLEIN F. (1884). Lectures on the Icosahedron and the Solution of Equations of the Fifth Degree, Cambridge University Press, Dover reprint, 1956, United Kingdom, UK.

KREYSZIG E. (1979). Advanced Engineering Mathematics, Book, 4th edition, Wiley and Sons, New York, NY, USA.

KUMMER E.E. (1836). On the Hypergeometric Series F (a, b; c; x), Journal für die reine und angewandte Mathematik, Crelle's Journal, Vol. 15, pp. 39-83.

LAKEHAL M., ACHOUR B. (2014). Computation of normal flow depth in an egg-shaped conduit using the rough model method, Larhyss Journal, No 19, pp. 101-113. (In French)

LAKEHAL M., ACHOUR B. (2017). New approach for the normal depth computation in a trapezoidal open channel using the rough model method, Larhyss Journal, No 32, pp. 269-284.

LAWSON C.L. (1961). Contributions to the Theory of Linear Least Maximum Approximations, Ph.D. Thesis, University of California, Los Angeles, USA, 198p.

NAKATSUKASA Y., SETE O., TREFTHEN L.N. (2018). The AAA algorithm for rational approximation, Society for Industrial and Applied Mathematics (SIAM) Journal on Scientific Computing, Vol. 40, Issue 3, pp. A1494-A1522.

PASSARE M., TSIKH A. (2002). Algebraic Equations and Hypergeometric Series, American Mathematical Monthly, Vol. 109, Issue 4, pp. 330-341.

POCHHAMMER L.A. (1890). On the expansion of the gamma function in series, Mathematical Annals, Vol. 37, pp. 470-489.

Proceedings of the Institution of Civil Engineers: Water Management, Vol. 166, pp. 199-206.

RAGHUNATH H.M. (2006). Hydrology: Principles, Analysis and Design, Book, 2nd Edition, Private New Age International Ltd., New Delhi, India, 463 pages.

RATHIE A.K., SWAMEE P.K. (2006). On explicit equations for normal depth, Journal of Hydrologic Engineering, American Society of Civil Engineers (ASCE), Vol. 11, Issue 6, pp. 527-532.

SEHTAL S., ACHOUR B. (2023). Normal depth computation in a vaulted rectangular channel using the rough model method (RMM), Larhyss Journal, No 54, pp. 193-216.

SHANG H., XU S., ZHANG K. (2020). Improvements to solutions for normal depth in multiple sections of tunnels, Flow Measurement and Instrumentation, Vol.73, Paper ID 101723.

SRIVASTAVA R. (2006). Discussion of “exact solutions for the normal depth problem” by Swamee P.K. and Rathie P.N., Journal of Hydraulic Research, Vol. 44, Issue 3, pp. 427-428.

SWAMEE P. K., RATHIE P.N. (2004). Exact solutions for normal depth problem, Journal of hydraulic Research, Vol. 42, Issue 5, pp. 543-550.

SWAMEE P.K. (1994). Normal Depth Equations for Irrigation Canals, Journal of Irrigation and Drainage Engineering, Vol. 120, No 5, pp. 942-948.

SWAMEE P.K., RATHIE A.K., OJHA C.S.P. (2000). Explicit equations for uniform flow in open channels, Journal of Hydrologic Engineering, American Society of Civil Engineers (ASCE), Vol. 5, Issue 4, pp. 414-420.

TREFETHEN L.N. (2013). Approximation Theory and Approximation Practice, 1st Edition, Society for Industrial and Applied Mathematics (SIAM), 318p.

TSCHIRNHAUS E.W.V. (1683). On the method of removing all intermediate terms from a given equation, Acta Eruditorum, Leipzig, Germany, pp. 204–211.

VATANKHAH A.R. (2012). Direct solutions for normal and critical depths in standard city-gate sections, Flow Measurement and Instrumentation, Vol. 28, pp. 16-21.

VATANKHAH A.R. (2015). Direct solutions for normal depth in parabolic and rectangular open channels using asymptotic matching technique, Flow Measurement and Instrumentation, Vol. 46, pp. 66-71.

VATANKHAH A.R., EASA S.M. (2011). Explicit solutions for critical and normal depths in channels with different shapes, Flow Measurement and Instrumentation, Vol. 22, No 1, pp. 43-49.

WHITTAKER E.T., WATSON G.N. (1927). A Course of Modern Analysis, 4th Edition, Cambridge University Press, United Kingdom, UK, pp. 125-138.

ZWILLINGER D. (2018). Standard mathematical tables and formulas, Chemical Rubber Company (CRC) Press.